Cellular Microbiology (2015) **17**(1), 79–104
doi:10.1111/cmi.12338
First published online 9 September 2014

Macrophage induced gelsolin in response to Group B *Streptococcus* (GBS) infection

Katia Fettucciari,[1]* Pamela Ponsini,[1] Camilla Palumbo,[2] Emanuela Rosati,[1] Roberta Mannucci,[3] Rodolfo Bianchini,[4,5] Andrea Modesti[2] and Pierfrancesco Marconi[1]
[1]*Department of Experimental Medicine, Perugia University, Perugia, Italy.*
[2]*Department of Clinical Sciences and Translational Medicine, Tor Vergata University, Rome, Italy.*
[3]*Department of Medicine, Laboratory of Image Analysis, Perugia University, Perugia, Italy.*
[4]*Research Program for Receptor Biochemistry and Tumor Metabolism, Laura Bassi Centre of Expertise Therapep, Salzburg University Clinic, Salzburg, Austria.*
[5]*Department of Pediatrics, Paracelsus Medical University, Muellner Hauptstrasse, Salzburg, Austria.*

Summary

Group B *Streptococcus* (GBS) has evolved several strategies to avoid host defences. We have shown that interaction of macrophages with GBS causes macrophage calpain activation, cytoskeletal disruption and apoptosis, consequences of intracellular calcium increase induced by membrane permeability alterations provoked by GBS-β-haemolysin. Open question remains about what effect calcium influx has on other calcium-sensing proteins such as gelsolin, involved in cytoskeleton modulation and apoptosis. Therefore we analysed the effect of GBS-III-COH31:macrophage interaction on gelsolin expression. Here we demonstrate that an early macrophage response to GBS-III-COH31 is a very strong gelsolin increase, which occurs in a time- and infection-ratio-dependent manner. This is not due to transcriptional events, translation events, protein turnover alterations, or protein-kinase activation, but to calcium influx, calpain activation and caspase-3 degradation. In fact, EGTA and PD150606 (calpain inhibitor) prevented gelsolin increase while BAF (caspase inhibitor) enhanced it. Since gelsolin increase is induced by highly β-haemolytic GBS-III-NEM316 and GBS-V-10/84, but not by weakly β-haemolytic GBS, or GBS-III-COH31 in conditions suppressing β-haemolysin expression/activity and the presence of dipalmitoylphosphatidylcholine (β-haemolysin inhibitor), GBS-β-haemolysin is solely responsible for gelsolin increase causing, through membrane permeability defects, calcium influx and calpain activation. Early gelsolin increase could represent a macrophage response to antagonize apoptosis since gelsolin knockdown increases macrophage susceptibility to GBS-induced apoptosis. This response seems to be GBS specific because macrophage apoptosis by Staurosporine or Cycloeximide does not induce gelsolin.

Received 22 March, 2013; revised 4 July, 2014; accepted 31 July, 2014. *For correspondence. E-mail katia.fettucciari@unipg.it; Tel. (+39) 75 5858124.

© 2014 John Wiley & Sons Ltd

Introduction

Streptococcus agalactiae (Group B *Streptococcus*, GBS) is the leading cause of serious invasive infections in human neonates and an emerging pathogen in adults, particularly the elderly and those with underlying chronic disease (Baker and Edwards, 1995; Maisey *et al*., 2008). The first step of GBS infection implies the interaction of GBS with the first line of host innate immune defence mechanisms especially macrophages (MΦ). The interaction of GBS with MΦ is extremely complex and results in: resistance to phagocytosis by MΦ through an antiphagocytic capsule which prevents opsonic complement-mediated and non-opsonic scavenger receptor A mediated phagocytosis (Rubens *et al*., 1987; Areschoug *et al*., 2008), invasion of MΦ and intracellular survival inside MΦ, with manipulation of MΦ antibacterial activity (Valentin-Weigand *et al*., 1996; Cornacchione *et al*., 1998; Maisey *et al*., 2008) and MΦ proinflammatory cytokine responses (Rosati *et al*., 1998), disruption of MΦ cytoskeleton (Fettucciari *et al*., 2011) and induction of MΦ apoptosis (Fettucciari *et al*., 2000; 2003; 2006) induced through activation of calpains, calcium-dependent proteases, as a consequence of a strong extracellular calcium (Ca^{2+}) influx in MΦ induced by GBS through β-haemolysin (Fettucciari *et al*., 2000; 2006; 2011). However, we do not know what other effects the strong increase of intracellular Ca^{2+} induced by GBS could have on MΦ and their response.

Alteration of intracellular Ca^{2+} homeostasis is of particular relevance during host cell infection by some pathogens

(TranVan Nhieu *et al*., 2004). In fact, Ca^{2+} signalling has been implicated in a wide range of bacterial infection processes, among which the respiratory burst, the control of gene expression – especially that leading to the expression and secretion of proinflammatory mediators – cytoskeletal reorganization and degradation, and induction of apoptosis (May and Machesky, 2001; TranVan Nhieu *et al*., 2004; Groves *et al*., 2008; Melendez and Tay, 2008). Ca^{2+} plays many different roles in these processes by affecting the actions of intracellular Ca^{2+}-sensing proteins, among which gelsolin, which in particular plays a crucial role in cytoskeletal modulation and apoptosis (May and Machesky, 2001; Belyi, 2002; Groves *et al*., 2008; Melendez and Tay, 2008; Li *et al*., 2012). Gelsolin is a Ca^{2+}-dependent and PI(4,5)P2-regulated cytoskeleton protein composed of six repeating domains of sequence (G1–6). Each domain contains a Ca^{2+} binding site and three distinct actin binding sites, two that bind to G-actin (G1 and G4–6) and one that binds to filaments (G2–3) (Kwiatkowski, 1999; McGough *et al*., 2003; Silacci *et al*., 2004; Li *et al*., 2012). The structural and functional activation of gelsolin is a two-step, three-state process strongly regulated by intracellular Ca^{2+} concentrations [Ca^{2+}]. In fact, at low [Ca^{2+}] gelsolin has a compact, globular, inactive structure while at increasing [Ca^{2+}] gelsolin opens up and by inducing a conformational change in the *C*-terminal half exposes actin binding sites on the N-terminal half (Kwiatkowski, 1999; Kiselar *et al*., 2003; McGough *et al*., 2003; Silacci *et al*., 2004; Ashish *et al*., 2007; Li *et al*., 2012). Gelsolin is an actin binding protein that has multiple pleiotropic actin regulatory activities (Kwiatkowski, 1999; Silacci *et al*., 2004; Li *et al*., 2012). In effect, severing, uncapping and binding actin filaments by this protein increases filament number and provide many free polymerizing ends so controlling actin assembly and disassembly. But gelsolin might dissolve the cortical actin cytoskeleton and allow receptor clustering and new localized actin polymerization. Interestingly, some evidence supports the idea that gelsolin regulates actin remodelling through Rac activation, which correlates with the ability of Rac to trigger the dissociation of gelsolin from actin filaments and the receptor preference indicated (Arcaro, 1998; Azuma *et al*., 1998; De Corte *et al*., 2002; Silacci *et al*., 2004; Li *et al*., 2012). Therefore, gelsolin by these actin regulatory activities is involved in cytoskeletal remodelling, phagocytosis and ion channel regulation (Kwiatkowski, 1999; McGough *et al*., 2003; Silacci *et al*., 2004; Li *et al*., 2012). In addition, gelsolin has both anti-apoptotic and pro-apoptotic functions depending on the different cell types, the specific tissues and the nature of the pathological conditions involved (Kothakota *et al*., 1997; Kwiatkowski, 1999; Koya *et al*., 2000; Kusano *et al*., 2000; Silacci *et al*., 2004; Li *et al*., 2012). Gelsolin is also involved in signal transduction, transcriptional regulation, epigenetic processes and there is now increasing evidence that it is a multifunctional regulator of cell metabolism involving multiple mechanisms independent of its actin regulatory functions (Kwiatkowski, 1999; Silacci *et al*., 2004; Spinardi and Witke, 2007; Li *et al*., 2012).

In the light of our previous results demonstrating the crucial role of GBS-induced Ca^{2+} influx on MΦ calpain activation, MΦ apoptosis and MΦ cytoskeleton disruption, effects that play a crucial role in GBS evasion of MΦ responses (Fettucciari *et al*., 2000; 2006; 2011), we investigated if the strong influx of extracellular Ca^{2+} in MΦ induced by GBS affects the expression of the Ca^{2+}-regulated protein, gelsolin and the consequences on MΦ : GBS interaction.

This study demonstrates that a very early MΦ response to the more β-haemolytic strains of GBS [GBS type III strain COH31 r/s (GBS-III-COH31), GBS type III strain NEM316 (GBS-III-NEM316), GBS type V strain NCTC10/84 (GBS-V-10/84)], is a strong gelsolin increase, which occurs in a time- and infection-ratio-dependent manner. Gelsolin increase is caused by Ca^{2+} influx, calpain activation and consequent caspase-3 degradation, and is not due to transcriptional events, translation events, protein turnover alterations, translocation from other subcellular compartments or protein-kinase activation. Finally results of gelsolin knockdown by small interfering RNA suggest that gelsolin increase contributes to counter the GBS induction of MΦ apoptosis.

Results

GBS-III-COH31 induces gelsolin increase in MΦ

In agreement with the results of our previous studies, GBS-III-COH31 in a time- and infection-ratio-dependent manner induces alterations in MΦ membrane permeability (Fettucciari *et al*., 2000; 2011; Fig. 1A), allowing a progressive strong influx of extracellular Ca^{2+} in MΦ (Fettucciari *et al*., 2000), which leads at 2 h to cytoskeletal disruption (Fettucciari *et al*., 2011; Fig. 1B). Since it is known that gelsolin, a multifunctional regulatory protein, is activated and regulated by [Ca^{2+}] (Kwiatkowski, 1999; Kiselar *et al*., 2003; Silacci *et al*., 2004; Ashish *et al*., 2007; Li *et al*., 2012) and, as above reported, the GBS-III-COH31 infection of MΦ leads to strong intracellular Ca^{2+} increase, we evaluated if the MΦ : GBS-III-COH31 interaction affects gelsolin expression.

To this end MΦ were infected with GBS-III-COH31 for 0.5, 1 and 2 h at three different MΦ : GBS infection ratios and the levels of gelsolin and β-actin (loading control) were analysed by Western blot. Western blot analysis showed that the levels of gelsolin increased in a time- and infection-ratio-dependent manner in MΦ after GBS-III-

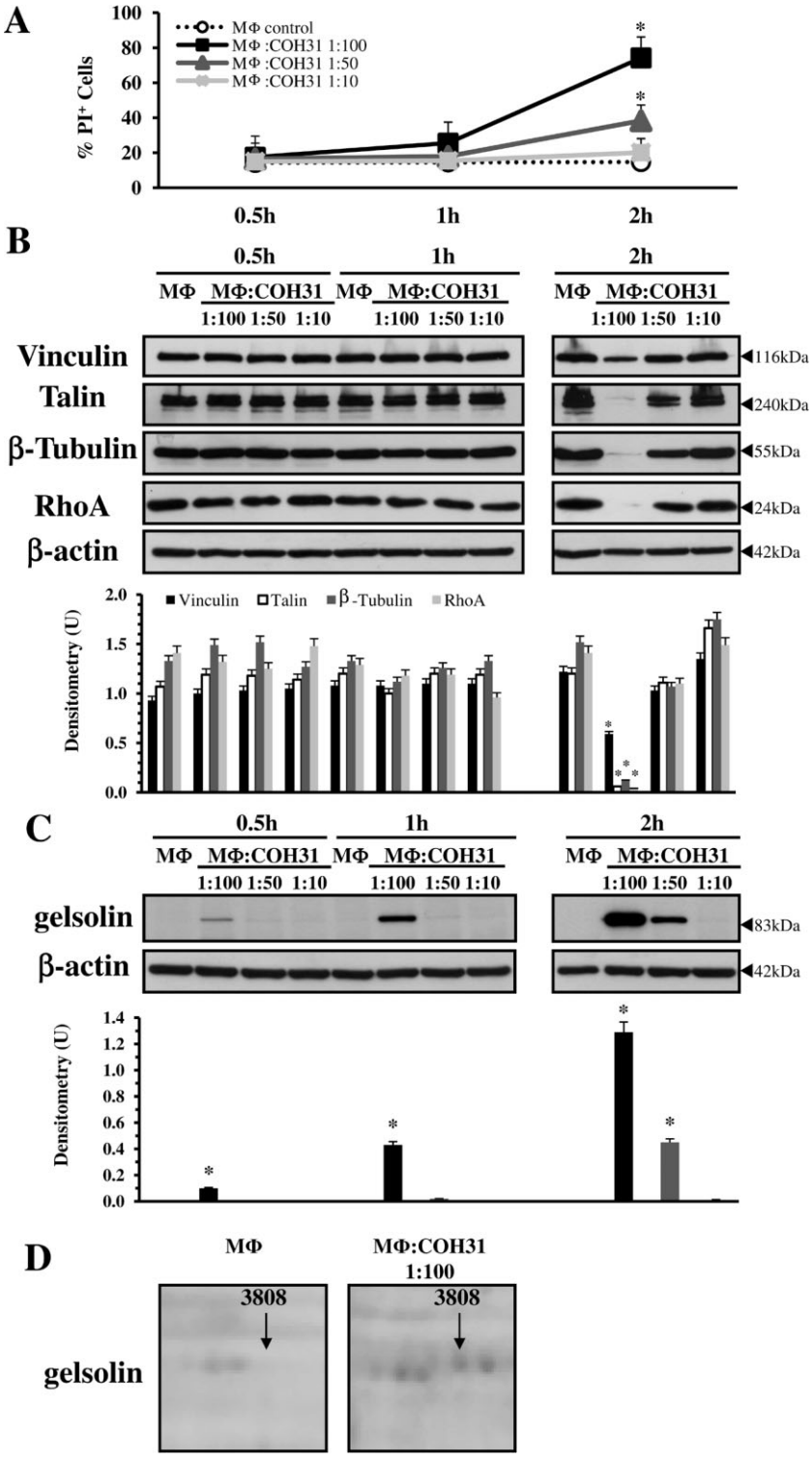

Fig. 1. Effect of MΦ : GBS-III-COH31 interaction on the expression of gelsolin.
A. Flow cytometry analysis. Percentage of PI+ cells was determined by PI uptake assay at flow cytometry in control MΦ and MΦ infected with GBS-III-COH31 at the indicated ratios, recovered at different times after infection. Data are means ± SD of six experiments done in triplicate. $^*P < 0.01$ GBS-infected MΦ versus control MΦ.
B. Western blot analysis of cytoskeletal protein expression. Lysates from control MΦ and MΦ infected with GBS-III-COH31 (MΦ : COH31) at the indicated ratios, prepared at the indicated times, were subjected to SDS-PAGE. The filters were cut around 80 kDa and 30 kDa. The top sections probed with anti-Vinculin, then stripped and reprobed with anti-Talin. The middle sections probed with anti-β-Tubulin, then stripped and reprobed with anti-β-actin. The bottom sections were probed with anti-RhoA.
C. Western blot analysis of gelsolin expression. Lysates from control MΦ and MΦ infected with GBS-III-COH31 (MΦ : COH31) at the indicated ratios, prepared at the indicated times, were subjected to SDS-PAGE. The filters were cut around 70 kDa, the top sections were probed with anti-gelsolin and the bottom sections were with anti-β-actin.
D. Proteomic analysis of gelsolin expression. Details from 2-DE maps were cropped to show one spot identified as gelsolin which was overexpressed in MΦ infected with GBS-III-COH31 (MΦ : COH31), compared to control MΦ. The spot was detected only in gels from MΦ infected with GBS-III-COH31.
B and C. The density of bands corresponding to each protein was evaluated by densitometric analysis. Densitometry units (U) were calculated relative to β-actin and values for the densitometric analyses obtained from four independent experiments. $^*P < 0.01$ GBS-infected MΦ versus control MΦ.

COH31 infection reaching the maximum at 2 h (Fig. 1C). GBS-III-COH31 at a ratio of 1:100 induced gelsolin expression in MΦ by approximately 0.1 densitometry units at 0.5 h of infection (Fig. 1C), 0.43 densitometry units at 1 h of infection (Fig. 1C) and 1.29 densitometry units at 2 h of infection (Fig. 1C), while in control MΦ the gelsolin expression was undetectable at all times examined. GBS-III-COH31 at a ratio of 1:50 induced gelsolin expression in MΦ by approximately 0.45 densitometry units only at 2 h infection (Fig. 1C). On the contrary GBS-III-COH31 at a

ratio of 1:10 induced no increase in gelsolin expression in MΦ at all times examined (Fig. 1C).

Gelsolin increase occurred already at 0.5 h and strongly increased at 1 h after GBS-III-COH31 infection of MΦ (Fig. 1C) times at which significant changes of intracellular [Ca^{2+}] were detected (Fettucciari *et al*., 2000; 2006) but no cytoskeleton disruption (Fettucciari *et al*., 2011; Fig. 1B) was found, indicating that gelsolin overexpression occurs before cytoskeletal degradation.

Unpublished results of proteomic analysis performed in our previous paper (Susta *et al*., 2010) on control MΦ and MΦ infected with GBS-III-COH31 at a ratio of 1:100 for 2 h showed that a spot identified as gelsolin was overexpressed in MΦ infected with GBS-III-COH31 but was undetectable in control MΦ (Fig. 1D) confirming the Western blot results.

Overall, these results indicate that GBS-III-COH31 induces a strong gelsolin increase in MΦ and that this is a very early event during MΦ : GBS interaction.

Gelsolin increase is independent of transcriptional, translational, protein-kinase and proteasome activity

In order to understand the mechanisms responsible for gelsolin increase we first investigated the role of transcription activity by quantitative real-time PCR (qRT-PCR). To this end we evaluated gelsolin mRNA content in control and GBS-infected MΦ at 2 h after infection, time at which we observed the higher gelsolin increase. No significant increase of gelsolin expression at mRNA level was observed with qRT-PCR in GBS-infected MΦ with respect to control MΦ (Fig. 2A).

Successively we investigated the role of de novo protein synthesis. MΦ were pretreated with 10 or 50 μg ml^{-1} Cycloheximide (CHX), an inhibitor of eukaryotic protein synthesis, (Fettucciari *et al*., 2000; Croons *et al*., 2007; Ji *et al*., 2010) for 1 h before infection with GBS-III-COH31 and gelsolin expression was analysed by Western blot. The ratio of gelsolin to loading control β-actin was used to monitor the relative levels of gelsolin on CHX-treatment. As shown in Fig. 2B, the gelsolin expression induced by GBS-III-COH31 was not significantly blocked by pretreatment with 10 or 50 μg ml^{-1} CHX. In fact, a similar level of gelsolin expression was observed in non-treated GBS-infected MΦ and GBS-infected MΦ treated with CHX at 10 or 50 μg ml^{-1}. Therefore the gelsolin increase in MΦ by GBS is not due to de novo protein synthesis.

To continue to explore the molecular mechanism implicated in the gelsolin increase by MΦ : GBS-III-COH31 interaction, since the fundamental functions of the signalling cascade in evoking cellular responses to external stimuli/infection are mediated by protein-kinases, we investigated the role of Staurosporine (STS), a potent inhibitor of protein-kinases that acts by competing with ATP in binding to the nucleotide-binding pocket, and has a broad activity across a variety of protein-kinases (Toledo and Lydon, 1997; Ji *et al*., 2010). MΦ were pretreated with 63 nM STS 1 h before infection with GBS-III-COH31 at a ratio of 1:100 for 2 h. The results showed that 63 nM STS does not significantly inhibit the gelsolin increase induced by GBS (Fig. 2C) indicating that gelsolin increase is not mediated by activation of protein-kinases.

Since the increased gelsolin expression is not due to transcriptional, translation or protein-kinase activity we initially looked whether gelsolin increase was caused by inhibition of proteasome activity by GBS that leads to altered turnover of gelsolin and its accumulation in MΦ. To this end we analysed, by Western blot, the accumulation of multiubiquitinylated proteins in GBS-infected MΦ (Paolini *et al*., 2001). As positive control to show accumulation of multiubiquitinylated proteins we used MΦ treated with 2 μM *clasto*-Lactacystin-β-lactone (*clasto*-Lactacystin) that inhibits proteasome activity in MΦ (Paolini *et al*., 2001; Fettucciari *et al*., 2006). We found an accumulation of high molecular weight protein-ubiquitin conjugates in *clasto*-Lactacystin treated MΦ (Fig. 2D) whereas GBS-infected MΦ, as control MΦ, showed no accumulation of multiubiquitinylated proteins (Fig. 2D). Therefore the gelsolin increase is not due to inhibition of MΦ proteasome activity by GBS.

Rather the observation that there is a build up of ubiquitinated proteins in control MΦ with respect to GBS-infected MΦ in Fig. 2D and in Fig. 3A leads to the hypothesized that this could be due to calpain activation induced by GBS. In fact, over ubiquitin proteasome pathway other cellular apparatuses such as calpains play significant roles in post-transcriptional processing and turnover of several cellular proteins (Coux *et al*., 1996; Goll *et al*., 2003; Zhou, 2004; Nandi *et al*., 2006). Moreover, it has been demonstrated in some experimental models that calpain activation increased total protein degradation and in particular calpain activation increased cytoplasmic proteolysis mediated by proteasome (Menconi *et al*., 2004; Smith and Dodd, 2007). Therefore, calpains activated by GBS could increase both total cytoplasmic proteolysis and proteolysis mediated by proteasome.

Proteasome inhibitors have been shown to stabilize proteins designated for degradation by proteasome (Coux *et al*., 1996; Patrick *et al*., 1998; Zhao *et al*., 2000). Since in other experimental models the gelsolin is efficiently degraded by the ubiquitin proteasomal pathway (Ni *et al*., 2008), inhibitors of the proteasome such as MG132 or *clasto*-Lactacystin are likely to increase the half-life ($t_{1/2}$) of this protein in MΦ. To examine the effect of proteasomal inhibitors on gelsolin stability we used two different proteasome inhibitors, MG132 and *clasto*-Lactacystin, and evaluated gelsolin expression at 2 h after infection

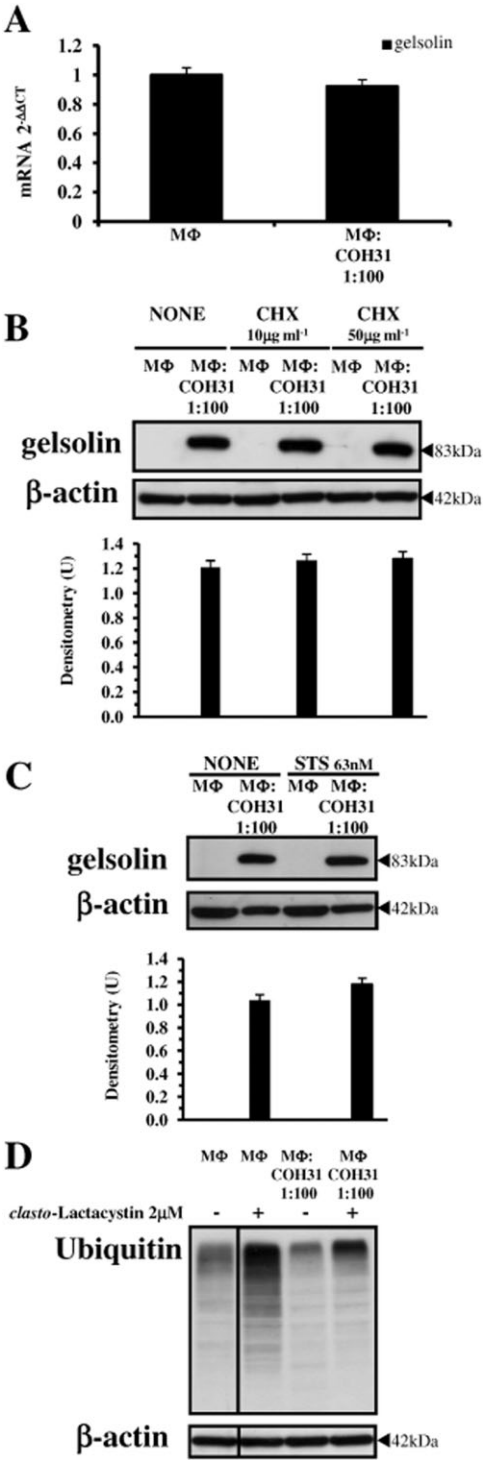

Fig. 2. Molecular mechanisms of gelsolin increase.
A. Analysis of gelsolin mRNA expression by qRT-PCR. Control MΦ and MΦ infected with GBS-III-COH31 at a ratio of 1:100 were subjected to qRT-PCR and data expressed as $2^{-\Delta\Delta Ct}$.
B. Effect of protein synthesis inhibitor on gelsolin expression by Western blot analysis. Lysates from non-treated MΦ, MΦ pretreated for 1 h with CHX (10 or 50 μg ml^{-1}), infected or not with GBS-III-COH31 (MΦ : COH31) at a 1:100 ratio for 2 h, were subjected to SDS-PAGE. The filter was probed with anti-gelsolin then stripped and reprobed with anti-β-actin.
C. Effect of protein-kinase inhibitor on gelsolin expression by Western blot analysis. Lysates from non-treated MΦ, MΦ pretreated for 1 h with STS (63 nM), infected or not with GBS-III-COH31 (MΦ : COH31) at a 1:100 ratio for 2 h, were subjected to SDS-PAGE. The filter was cut around 70 kDa and the top probed with anti-gelsolin, while the bottom was probed with anti-β-actin.
D. Western blot analysis of multiubiquitinylated proteins. Lysates from non-treated MΦ, MΦ pretreated for 1.5 h with *clasto*-Lactacystin (2 μM), infected or not with GBS-III-COH31 (MΦ : COH31) at a 1:100 ratio for 2 h, were subjected to SDS-PAGE. The filter was probed with anti-Ubiquitin, then stripped and reprobed with anti-β-actin. Vertical lines in blots indicate repositioned gel lanes.
B and C. The density of the bands corresponding to gelsolin was evaluated by densitometric analysis. Densitometry units (U) were calculated relative to β-actin and values for the densitometric analyses obtained from four independent experiments.

and 5 h after infection (2 h infection plus 3 h incubation with antibiotics). Since β-actin at 5 h after infection begins to decrease in GBS-infected MΦ (Fig. 3A, right panel) to monitor the relative levels of gelsolin in kinetics after proteasome inhibitor treatment we used Manganese Superoxide Dismutase (MnSOD) as loading control. The results obtained show that at all times examined the level of gelsolin in GBS-infected MΦ pretreated for 1.5 h with *clasto*-Lactacystin (2 μM) or MG132 (5 μM) remain the same as that of non-treated GBS-infected MΦ, indicating that in our experimental model both *clasto*-Lactacystin and MG132 do not stabilize gelsolin (Fig. 3A, upper panels). Proteasome activity is efficiently inhibited by pretreatment of MΦ with *clasto*-Lactacystin (2 μM) or MG132 (5 μM) as demonstrated by accumulation of multiubiquitinylated proteins in MΦ pretreated with proteasome inhibitors, at all times examined (Fig. 3A, middle panels). These data further indicate that proteasome is not involved in gelsolin turnover in GBS-infected MΦ.

To rule out definitively the proteasome involvement in gelsolin turnover we also evaluated the gelsolin $t_{1/2}$ by CHX treatment and simultaneous treatment with the proteasomal inhibitor *clasto*-Lactacystin (Zhao *et al.*, 2000; Zhou, 2004). To this end MΦ were pretreated for 1.5 h with 2 μM *clasto*-Lactacystin and simultaneously with 50 μg ml^{-1} CHX, then infected with GBS-III-COH31 in the presence of *clasto*-Lactacystin and CHX which were maintained in the medium all during the experiment. Then gelsolin expression was analysed at 2 h after infection and 8 h after infection (2 h infection plus 6 h incubation with antibiotics) by Western blot. For the same reasons described above, to monitor the relative levels of gelsolin in kinetics after proteasome and CHX treatment we used as loading control MnSOD.

The results obtained showed that a weak gelsolin expression was detectable in untreated MΦ at 8 h of

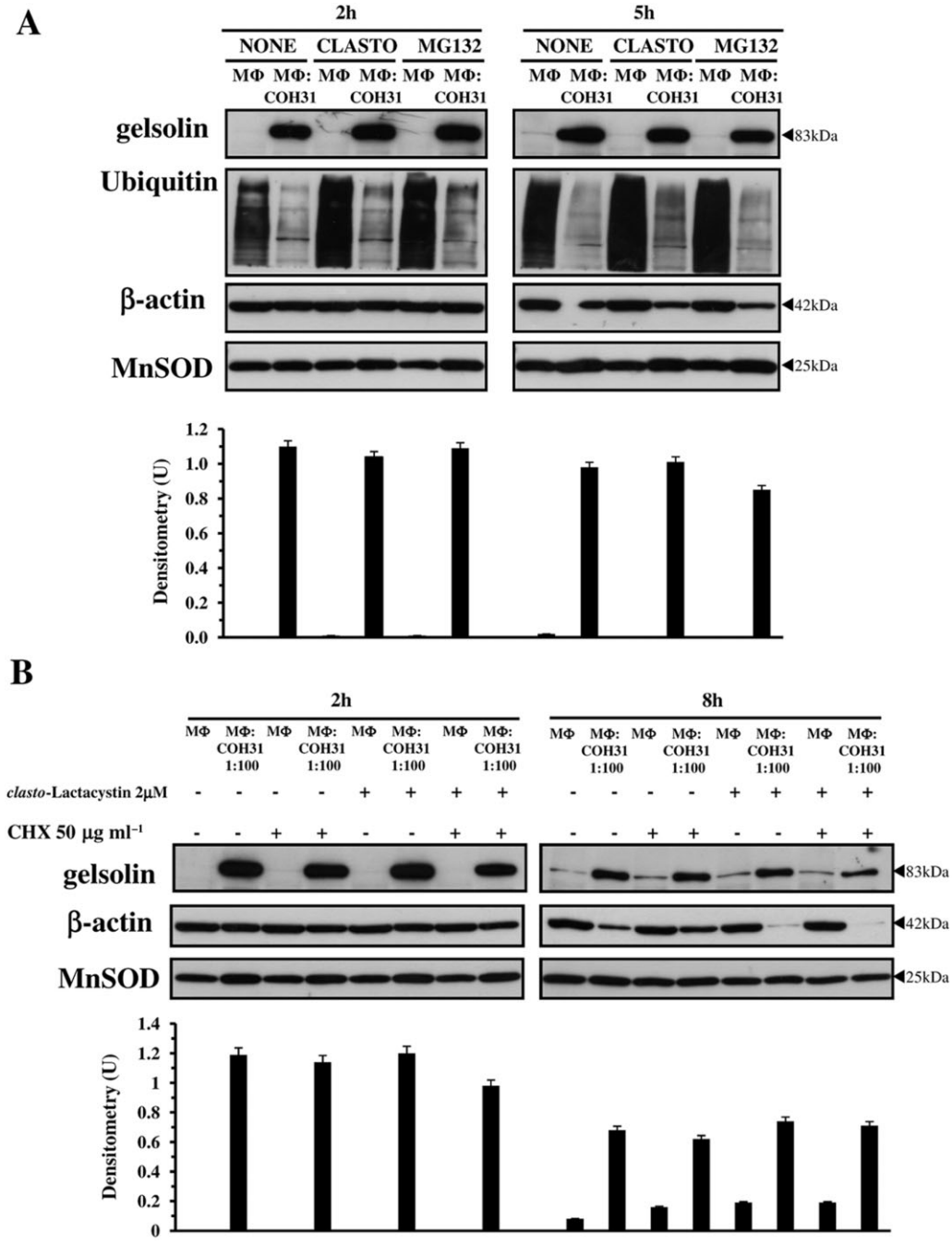

Fig. 3. Effect of proteasome on gelsolin turnover.
A. Western blot analysis of gelsolin and multiubiquitinylated proteins after proteasome inhibitor treatment. Lysates from non-treated MΦ, MΦ pretreated for 1.5 h with *clasto*-Lactacystin (2 μM) or MG132 (5 μM), infected or not with GBS-III-COH31 (MΦ : COH31) at a 1:100 ratio, prepared at 2 h after infection and at 5 h after infection (2 h infection plus 3 h incubation with antibiotics), were subjected to SDS-PAGE. The filters were cut around 60 kDa and the top sections probed with anti-gelsolin then stripped and reprobed with anti-Ubiquitin, while the bottom sections were probed with anti-β-actin then stripped and reprobed with anti-MnSOD.
B. Effect of simultaneous treatment with protein synthesis inhibitor and proteasome inhibitor on gelsolin expression by Western blot analysis. Lysates from non-treated MΦ, MΦ pretreated for 1.5 h with CHX (50 μg ml^{-1}), MΦ pretreated for 1.5 h with *clasto*-Lactacystin (2 μM), MΦ pretreated for 1.5 h simultaneously with *clasto*-Lactacystin (2 μM) and CHX (50 μg ml^{-1}), infected or not with GBS-III-COH31 (MΦ : COH31) at a 1:100 ratio, prepared at 2 h after infection and at 8 h after infection (2 h infection plus 6 h incubation with antibiotics), were subjected to SDS-PAGE. The filters were cut around 70 kDa and the top sections probed with anti-gelsolin, while the bottom sections were probed with anti-β-actin then stripped and reprobed with anti-MnSOD.
A and B. The density of the bands corresponding to gelsolin was evaluated by densitometric analysis. Densitometry units (U) were calculated relative to MnSOD and values for the densitometric analyses obtained from three independent experiments.

incubation (Fig. 3B, upper right panel) and although these results seem in contrast with undetectable gelsolin expression in untreated MΦ at 2 h, we think that this could be due to the fact that with the further time of incubation MΦ adhere more strongly to the substrate and this could lead to cytoskeleton reorganization that causes slightly changes in gelsolin expression. However prolonging the time of incubation (24 h) the gelsolin expression in untreated MΦ remain the same of that observed at 8 h of incubation (data not shown).

More important the results of CHX inhibition experiments showed also that gelsolin had a long $t_{1/2}$. In fact, in these experiments we were unable to determine gelsolin $t_{1/2,}$ as we found a similar level of gelsolin in CHX-treated GBS-infected MΦ and non-treated GBS-infected MΦ at all times examined (Fig. 3B, upper panels). Furthermore the gelsolin expression induced by GBS-III-COH31 was not affected by simultaneous treatment with CHX and *clasto*-Lactacystin for all the course of the experiment. In fact, a similar level of gelsolin expression was observed in non-treated GBS-infected MΦ and in GBS-infected MΦ treated simultaneously with 50 μg ml^{-1} CHX and 2 μM *clasto*-Lactacystin, at all times examined (Fig. 3B, upper panels). These data definitively confirm that gelsolin turnover in GBS-infected MΦ is not regulated by proteasome.

Gelsolin increase is not due to redistribution by subcellular compartments

It is known that studying the proteins that associate with and regulate the actin cytoskeleton has been traditionally difficult. To prepare whole cell lysates we used a modified Radioimmunoprecipitation assay (RIPA) lysis buffer which contains three different detergents (SDS; Triton X-100, sodium deoxycholate) so allowing the recovery also of cytoskeletal-associated proteins. However, to rule out that gelsolin may be in a subcellular compartment which is typically masked in conventional methods of Western blot analysis of whole cell lysates, we used the EMD Millipore ProteoExtract® Cytoskeleton Enrichment and Isolation Kit. This kit greatly increases the ability to detect and study the low abundance actin-associated proteins allowing the retention of focal adhesion and actin-associated proteins while removing soluble cytoplasmic and nuclear proteins from the cell. To this end MΦ were infected with GBS-III-COH31 for 1 h and 2 h at two different MΦ : GBS infection ratios and the levels of gelsolin, vimentin (loading control for cytoskeletal fraction), glyceraldehyde-3-phosphate dehydrogenase (GAPDH; loading control for nuclear and soluble fractions), and β-actin (loading control for all fractions since GAPDH was downmodulated by GBS) were analysed in the cytoskeletal, soluble and nuclear fraction by Western blot. Gelsolin was detected in both the soluble

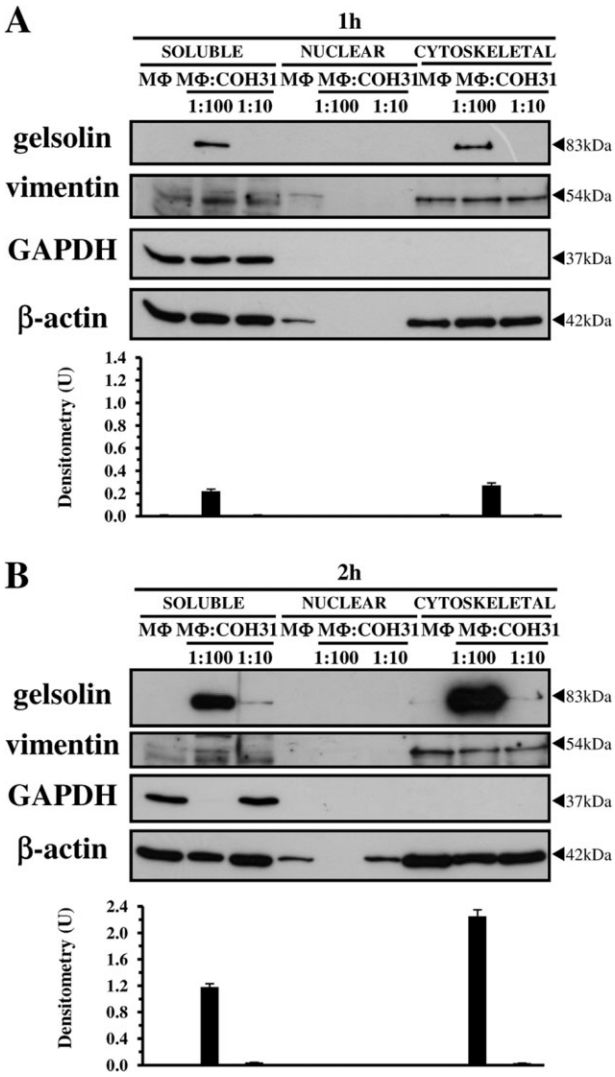

Fig. 4. Analysis of gelsolin expression in cytoskeletal, soluble or nuclear subfraction.
Cytoskeletal, soluble or nuclear subfraction from control MΦ, MΦ infected with GBS-III-COH31 (MΦ : COH31) at the indicated ratios, prepared at 1 h after infection (A) and 2 h after infection (B), were subjected to SDS-PAGE. The filters were probed with anti-gelsolin, then stripped and reprobed with anti-vimentin (loading control for the cytoskeletal fraction), then stripped and reprobed with anti-GAPDH (loading control for the soluble and nuclear fraction) then stripped and reprobed with anti-β-actin.
A and B. The density of the bands corresponding to gelsolin was evaluated by densitometric analysis. Densitometry units (U) were calculated relative to β-actin and values for the densitometric analyses obtained from three independent experiments.

and cytoskeletal fraction of MΦ infected with GBS-III-COH31 for 1 h at a MΦ : GBS ratio of 1:100 with a similar level of expression (Fig. 4A) and a strong increase in the cytoskeletal fraction of MΦ infected with GBS-III-COH31 for 2 h at a ratio 1:100 (Fig. 4B). In contrast gelsolin was not found in any subcellular fraction of control MΦ at all times examined (Fig. 4). While in MΦ infected with

GBS-III-COH31 at a ratio of 1:10 gelsolin was detected in both the soluble and cytoskeletal fraction at very low levels only at 2 h after infection (Fig. 4B).

Ca^{2+} is critical for gelsolin increase

Since, as previously reported GBS-III-COH31 induces a strong increase of intracellular Ca^{2+} in MΦ (Fettucciari *et al.*, 2000; 2006) and gelsolin is a Ca^{2+}-regulated protein (Kwiatkowski, 1999; McGough *et al.*, 2003; Silacci *et al.*, 2004; Li *et al.*, 2012), to study the involvement of Ca^{2+} in gelsolin increase induced by MΦ : GBS-III-COH31 interaction, we analysed the effect of the extracellular Ca^{2+} chelator, EGTA. MΦ were infected or not with GBS-III-COH31 at a MΦ : GBS infection ratio of 1:100 in the presence of 1 mM EGTA in RPMI-1640 medium (containing Ca^{2+} and Mg^{2+}) with 10% fetal bovine serum (FBS) at pH 7.3 for 2 h. EGTA at 1 mM strongly inhibited gelsolin increase by GBS-III-COH31 in MΦ (Fig. 5A). Adding EGTA in RPMI-1640 medium (containing Ca^{2+} and Mg^{2+}) with 10% FBS at pH 7.3 did not affect, MΦ viability which remained at 98–99% as evaluated by Trypan blue assay (Table 1), and MΦ adherence/morphology. In fact, by analysis of MΦ monolayers treated or not with EGTA infected or not with GBS-III-COH31 by inverted microscope controlled by cooled camera, no changes in cell morphology or adherence were observed between non-treated MΦ and EGTA-treated MΦ (Fig. 5B), or between GBS-infected non-treated MΦ and GBS-infected EGTA-treated MΦ. Significant changes were observed between control MΦ treated or not and GBS-infected MΦ treated or not (Fig. 5B) likely due to MΦ cytoskeletal disruption by GBS (Fig. 1B).

To further demonstrate that only extracellular Ca^{2+} is responsible for gelsolin increase, without the emptying of intracellular Ca^{2+} stores, we used the intracellular Ca^{2+} chelator [1,2-Bis(2-aminophenoxy)ethane-N,N,N′, N′-tetraacetic acid tetrakis(acetoxymethyl ester), BAPTA/AM]. MΦ were pretreated with 15 μM BAPTA/AM for 1 h then infected or not with GBS-III-COH31 at a MΦ : GBS infection ratio of 1:100 in the presence of BAPTA/AM in RPMI-1640 medium (containing Ca^{2+} and Mg^{2+}) with 10% FBS at pH 7.3 for 2 h. BAPTA/AM did not reduce gelsolin increase induced by GBS-III-COH31 in MΦ (Fig. 5C), thus demonstrating that the emptying of intracellular Ca^{2+} stores, is not involved in gelsolin increase.

Although EGTA preferentially binds to Ca^{2+} it can be considered a general chelator of divalent ions such as Mg^{2+}. Therefore, to show the specificity of EGTA for Ca^{2+} in gelsolin increase and definitively demonstrate that reduction of gelsolin by EGTA is due to influx of extracellular Ca^{2+}, we performed experiments by addition of an excess of $CaCl_2$ or $MgCl_2$ during incubation with EGTA in RPMI-1640 medium (containing Ca^{2+} and Mg^{2+}) with 10% FBS at pH 7.3. The inhibition of gelsolin increase by EGTA in GBS-infected MΦ can be reversed by addition of an excess of $CaCl_2$ but not $MgCl_2$ during incubation with EGTA (Fig. 5D). However, addition of an excess of $CaCl_2$ alone in control MΦ did not induce gelsolin increase (Fig. 5D). Therefore, these results showing that gelsolin increase was inhibited in the presence of EGTA and restored only by $CaCl_2$ demonstrated that GBS-induced gelsolin increase was caused by extracellular Ca^{2+} influx.

Calpain activation and caspase degradation are involved in gelsolin increase

Although the ubiquitin proteasome pathway constitutes the bulk of regulated cytoplasmic proteolysis, in most cases other cellular apparatuses, such as calpains, lysosome, and caspases also play significant roles in post-transcriptional processing and turnover of specific cellular proteins (Coux *et al.*, 1996; Carafoli and Molinari, 1998; Ciechanover, 1998; Pillay *et al.*, 2002; Goll *et al.*, 2003; Zhou, 2004; Nandi *et al.*, 2006; Bhatia *et al.*, 2013).

Fig. 5. Extracellular Ca^{2+} is responsible of gelsolin increase.
A. Effect of EGTA on gelsolin expression by Western blot analysis. Lysates from non-treated MΦ, MΦ treated with EGTA (1 mM), infected or not with GBS-III-COH31 (MΦ : COH31) at a 1:100 ratio for 2 h, were subjected to SDS-PAGE. The filter was cut around 70 kDa and the top probed with anti-gelsolin, while the bottom was probed with anti-β-actin.
B. Microscope analysis of effect of EGTA on MΦ adherence and morphology. Control MΦ, MΦ infected or not with GBS-III-COH31 (MΦ : COH31) at a 1:100 ratio for 2 h, MΦ treated with EGTA (1 mM), MΦ treated with EGTA (1 mM) infected with GBS-III-COH31 (MΦ EGTA : COH31) at a 1:100 ratio for 2 h, were analysed by Olympus IX51 microscope and images collected by Spot-2 cooled camera. Images are representative of three independent experiments.
C. Effect of BAPTA/AM on gelsolin expression by Western blot analysis. Lysates from non-treated MΦ, MΦ pretreated for 1 h with 15 μM BAPTA/AM (BAPTA), infected or not with GBS-III-COH31 (MΦ : COH31) at a 1:100 ratio for 2 h, were subjected to SDS-PAGE. The filter was cut around 70 kDa and the top probed with anti-gelsolin, while the bottom was probed with anti-β-actin.
D. Analysis of effect of addition of an excess of $CaCl_2$ or $MgCl_2$ during incubation with EGTA on gelsolin expression by Western blot analysis. Lysates from non-treated MΦ, MΦ treated with EGTA (1 mM), MΦ treated with EGTA (1 mM) and addition of 1 mM $CaCl_2$, MΦ treated with EGTA (1 mM) and addition of 1 mM $MgCl_2$, infected or not with GBS-III-COH31 (MΦ : COH31) at a 1:100 ratio for 2 h, were subjected to SDS-PAGE. The filter was cut around 70 kDa and the top probed with anti-gelsolin, while the bottom was probed with anti-β-actin.
A, C and D. The density of the bands corresponding to gelsolin was evaluated by densitometric analysis. Densitometry units (U) were calculated relative to β-actin and values for the densitometric analyses obtained from four independent experiments. *$P < 0.01$ GBS-infected treated MΦ versus GBS-infected non-treated MΦ.

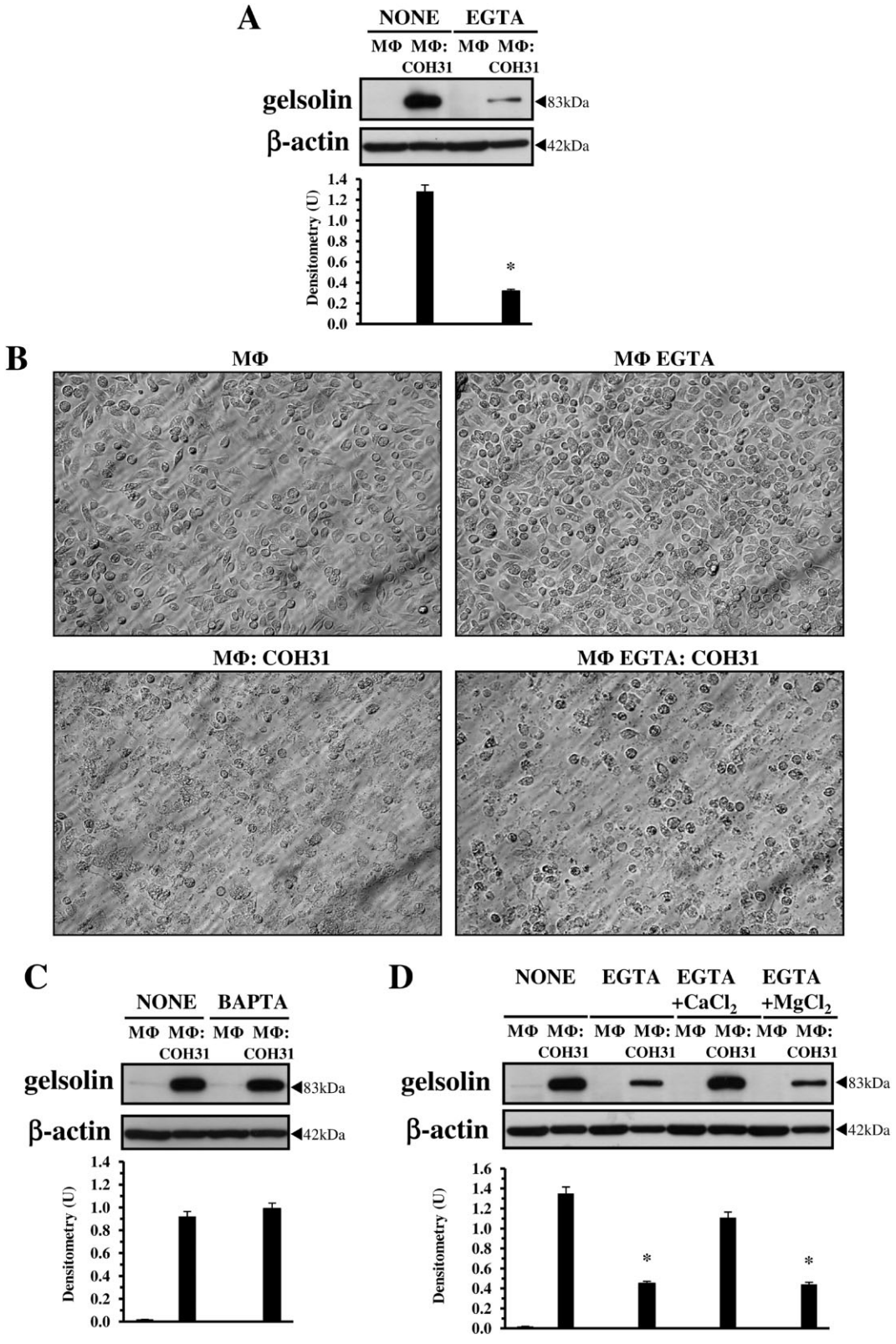
A
NONE
EGTA
MΦ
MΦ: COH31
MΦ
MΦ: COH31
gelsolin
β-actin
83kDa
42kDa
Densitometry (U)
1.4
1.2
1.0
0.8
0.6
0.4
0.2
0.0
*
B
MΦ
MΦ EGTA
MΦ: COH31
MΦ EGTA: COH31
C
NONE
BAPTA
MΦ
MΦ: COH31
MΦ
MΦ: COH31
gelsolin
β-actin
83kDa
42kDa
Densitometry (U)
1.4
1.2
1.0
0.8
0.6
0.4
0.2
0.0
D
NONE
EGTA
EGTA +CaCl2
EGTA +MgCl2
MΦ
MΦ: COH31
MΦ
MΦ: COH31
MΦ
MΦ: COH31
MΦ
MΦ: COH31
gelsolin
β-actin
83kDa
42kDa
Densitometry (U)
1.6
1.4
1.2
1.0
0.8
0.6
0.4
0.2
0.0
*
*

Table 1. Effect of EGTA on MΦ viability.

Treatment[a]	Total cell number × 10^5 ml^{-1}[b]
MΦ non-treated	29.8 (± 0.18)
MΦ : GBS-III-COH31	29.2 (± 0.22)
MΦ EGTA	29.4 (± 0.17)
MΦ EGTA : GBS-III-COH31	29.3 (± 0.20)

a. MΦ were infected or not with GBS-III-COH31 at a 1:100 ratio for 2 h in the presence or not of EGTA 1 mM.
b. At 2 h after infection, the cells were recovered as described in *Experimental procedures* and the total number of cells was determined by Trypan blue assay. The data are means ± SD of four experiments performed in triplicate.

We previously demonstrated that GBS infection induces in MΦ an influx of extracellular Ca^{2+} which is responsible for calpain activation (Fettucciari *et al*., 2006; 2011). To determine if gelsolin increase is affected by calpains, we examined the effect of a highly selective inhibitor of the μ- and m-calpain, which acts on the Ca^{2+} binding site, [3-(4-Iodophenyl)-2-mercapto-(Z)-2-propenoic acid, PD150606] (Wang *et al*., 1996; Carafoli and Molinari, 1998; Goll *et al*., 2003; Fettucciari *et al*., 2006), on MΦ gelsolin increase induced by GBS-III-COH31. To confirm the inhibition of calpains by PD150606, since a marker for the activation of calpains is the cleavage of α-spectrin into 150 and 145 kDa breakdown products (BP) (Wang *et al*., 1996; Goll *et al*., 2003; Fettucciari *et al*., 2006), we re-examined by Western blot the effect of PD150606 on α-spectrin cleavage induced by GBS-III-COH31. The results obtained show that the pretreatment of MΦ with 100 μM of PD150606 prevented the formation of 145 kDa α-spectrin BP induced by GBS-III-COH31 in MΦ (Fig. 6A), confirming that GBS-III-COH31 activates calpains and PD150606 inhibits their activation (Fig. 6A) and more important, the pretreatment of MΦ with 100 μM of PD150606 strongly reduces the gelsolin increase induced by GBS-III-COH31 (Fig. 6B), thus indicating that gelsolin increase is also due to calpain activation.

To investigate whether other proteases in particular lysosomal cathepsins are involved in MΦ gelsolin increase induced by GBS-III-COH31, we evaluated the effect of: i) the cathepsin B inhibitor IV (CA-074 Me), ii) the inhibitor of all lysosomal cathepsins, ammonium chloride (NH_4Cl), iii) the cathepsin D inhibitor (Pepstatin A). No inhibition or increase of gelsolin expression levels was observed with CA-074 Me (10 μM), NH_4Cl (10 mM) or Pepstatin A (10 μM) (Fig. 6C). This indicates that MΦ gelsolin increase is not due to the proteolytic activity of cathepsins.

Since it is well known that gelsolin is cleaved by caspase-3 (Kothakota *et al*., 1997; Jänicke *et al*., 1998; Kwiatkowski, 1999; Azuma *et al*., 2000; Koya *et al*., 2000; Silacci *et al*., 2004; Li *et al*., 2012), and we previously demonstrated that GBS cleave caspase-3 and -7 by calpain activation (Fettucciari *et al*., 2006), gelsolin increase in GBS-infected MΦ may be due to post-translational regulation based on reduced degradation of gelsolin owing to caspase degradation. To this end we analysed more rigorously the effect of boc-Asp(OMe)-fluoromethylketone (BAF), a broad spectrum caspase inhibitor, on gelsolin expression by Western blot and always by Western blot re-evaluated caspase-3 cleavage in MΦ infected with GBS-III-COH31 at a ratio of 1:100 for 2 h and the effect of calpain inhibitor, PD150606.

The analysis of caspase-3 expression confirms our previous results (Fettucciari *et al*., 2006) indicating that GBS-III-COH31 cleaves caspase-3 in MΦ (Fig. 7A) and PD150606, inhibits both the caspase-3 cleavage (Fig. 7A) and gelsolin increase (Figs 6B and 7A). Moreover we found that caspase inhibitory activity of BAF (25 μM) further increases the levels of gelsolin induced by GBS-III-COH31 in MΦ (Fig. 7B), without affecting caspase-3 expression levels in control and GBS-infected MΦ (Fig. 7C), indicating that in our model caspase-3 is involved in gelsolin increase. Therefore the demonstration that gelsolin increase was prevented by calpain inhibition which inhibited caspase-3 cleavage together with the observation that gelsolin increase was enhanced by caspase inhibitor BAF, indicates that gelsolin increase in GBS-infected MΦ involves altered degradation of gelsolin for lack of caspase-3.

Overall, these data indicate that gelsolin increase in MΦ induced by GBS-III-COH31 requires influx of extracellular Ca^{2+}, calpain activation mediated by Ca^{2+} influx, and caspase-3 degradation.

Confocal microscopy analysis of gelsolin expression in GBS-III-COH31 infected MΦ

Control MΦ and MΦ infected with GBS-III-COH31 at a ratio of 1:100 for 2 h, were triple-labelled using Alexa Fluor 488 phalloidin to detect F-actin, an Alexa Fluor 568-labelled goat anti-mouse secondary antibody (Ab) to detect gelsolin, and DAPI to visualized nuclei, and observed by confocal microscopy (Nikon Instruments, Amsterdam, Netherlands, C1 on Eclipse Ti; EZC1 software).

As illustrated in Fig. 8 top panels, control MΦ showed a very weak immunostaining for gelsolin, whereas many MΦ infected with GBS-III-COH31 were characterized by a strong and diffused gelsolin immunostaining. Conversely, no major differences in F-actin staining were detected between non-infected and infected MΦ (Fig. 8, top panels). Moreover, the GBS-induced increase of gelsolin immunolabelling was reduced by pretreatment with the calpain inhibitor PD150606 (100 μM) (Fig. 8, middle panels) and prevented by treatment with the Ca^{2+}

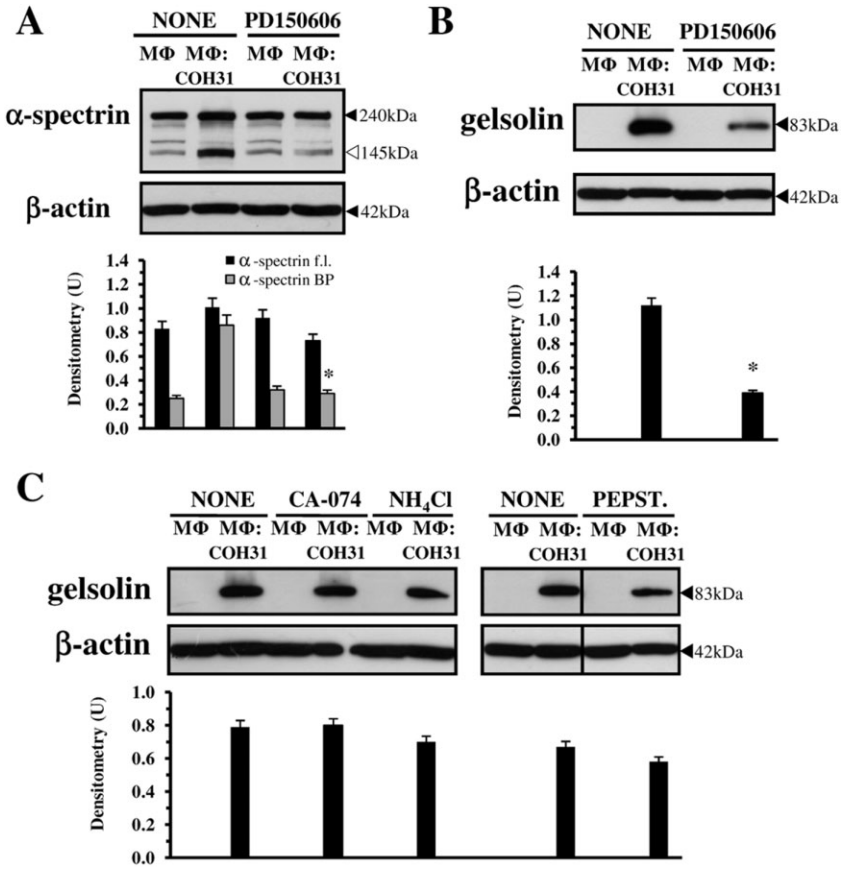

Fig. 6. PD150606 inhibited gelsolin increase while cathepsin inhibitors did not.
A. Effect of PD150606 on α-spectrin cleavage by Western blot analysis. Lysates from non-treated MΦ, MΦ pretreated for 1 h with PD150606 (100 μM), infected or not with GBS-III-COH31 (MΦ : COH31) at a 1:100 ratio for 2 h, were subjected to SDS-PAGE. The filter probed with anti-α-spectrin then stripped and reprobed with anti-β-actin. Intact protein (solid arrow) and BP (open arrow) are indicated.
B. Effect of PD150606 on gelsolin expression by Western blot analysis. Lysates from non-treated MΦ, MΦ pretreated for 1 h with PD150606 (100 μM), infected or not with GBS-III-COH31 (MΦ : COH31) at a 1:100 ratio for 2 h, were subjected to SDS-PAGE. The filter was cut around 70 kDa and the top probed with anti-gelsolin, while the bottom was probed with anti-β-actin.
C. Effect of cathepsin inhibitors on gelsolin expression by Western blot analysis. Lysates from non-treated MΦ, MΦ pretreated for 1.5 h with CA-074 Me (10 μM), MΦ pretreated for 1.5 h with NH_4Cl (10 mM), and MΦ pretreated for 18 h with Pepstatin A (10 μM), infected or not with GBS-III-COH31 (MΦ : GBS) at a 1:100 ratio for 2 h, were subjected to SDS-PAGE. The filters were cut around 70 kDa and the top sections probed with anti-gelsolin, while the bottom sections were probed with anti-β-actin. Vertical lines in blots in right panel indicate repositioned gel lanes.
A–C. The density of the bands corresponding to gelsolin, α-spectrin f.l., α-spectrin BP was evaluated by densitometric analysis. Densitometry units (U) were calculated relative to β-actin and values for the densitometric analyses obtained from four independent experiments. $*P < 0.01$ GBS-infected treated MΦ versus GBS-infected non-treated MΦ.

chelator, EGTA (1 mM) (Fig. 8, bottom panels), in agreement with the results of Western blot analysis.

These findings confirm at cellular level that GBS-III-COH31 induces gelsolin increase in MΦ by extracellular Ca^{2+} influx and calpain activation.

GBS β-haemolysin is involved in gelsolin increase

In a further series of experiments we analysed the possible microbial factor/s involved in MΦ gelsolin increase after GBS interaction. GBS has a pluripotent virulence factor, the β-haemolysin, strictly bound to the cell surface, highly unstable when released in culture supernatants, requiring metabolic activity for its production, and in virtue of its pore-forming-like activity against the eukaryotic cell membrane (Nizet *et al.*, 1996; Valentin-Weigand *et al.*, 1997; Fettucciari *et al.*, 2000; 2006; Nizet, 2002; Hensler *et al.*, 2008; Maisey *et al.*, 2008), causes plasma membrane permeability defects which allow a massive Ca^{2+} influx in MΦ and in other different cell types (Valentin-Weigand *et al.*, 1997; Fettucciari *et al.*, 2000; 2006; Hensler *et al.*, 2008). Since in our model, as reported above, the MΦ gelsolin increase was mediated by extracellular Ca^{2+} influx we examined the possibility

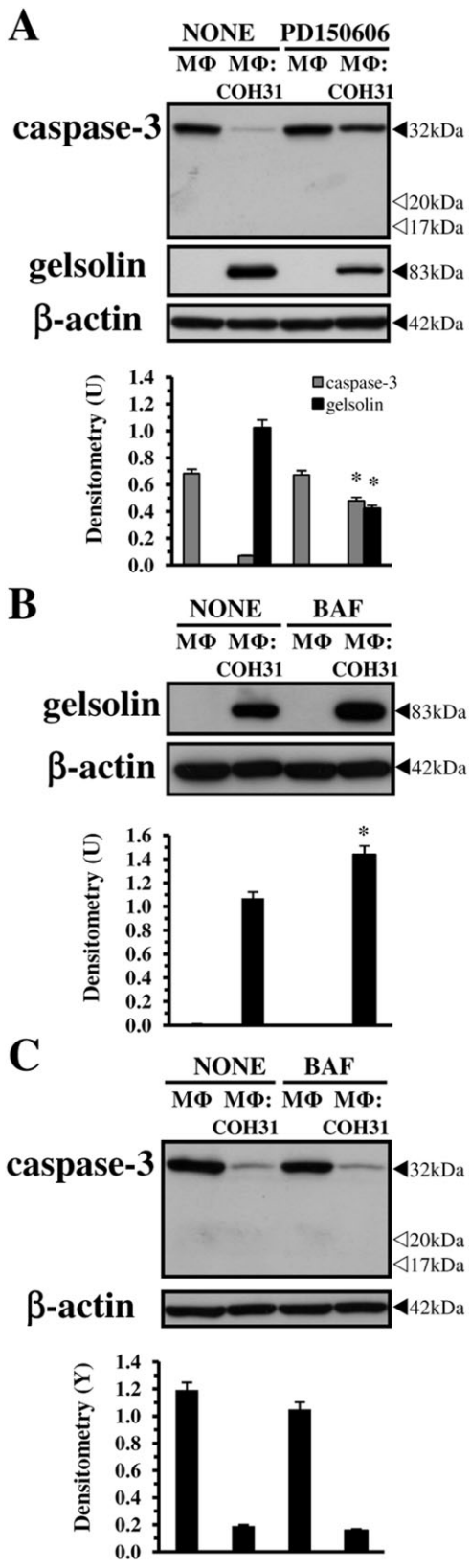

Fig. 7. Caspase-3 degradation mediated by calpains is involved in gelsolin increase.
A. Western blot analysis of caspase-3 and gelsolin expression and effect of PD150606. Lysates from non-treated MΦ, MΦ pretreated for 1 h with PD150606 (100 μM), infected or not with GBS-III-COH31 (MΦ : COH31) at a 1:100 ratio for 2 h, were subjected to SDS-PAGE. The filter was cut around 70 kDa and the top probed with anti-gelsolin, while the bottom probed with anti-caspase-3 then stripped and reprobed with anti-β-actin. Intact protein (solid arrow) and BP (open arrow) are indicated.
B. Effect of BAF on gelsolin expression by Western blot analysis. Lysates from non-treated MΦ, MΦ pretreated for 2 h with BAF (25 μM), infected or not with GBS-III-COH31 (MΦ : COH31) at a 1:100 ratio for 2 h, were subjected to SDS-PAGE. The filter was cut around 70 kDa and the top probed with anti-gelsolin, while the bottom was probed with anti-β-actin.
C. Effect of BAF on caspase-3 expression by Western blot analysis. Lysates from non-treated MΦ, MΦ pretreated for 2 h with BAF (25 μM), infected or not with GBS-III-COH31 (MΦ : COH31) at a 1:100 ratio for 2 h, were subjected to SDS-PAGE. The filter was cut around 70 kDa and the bottom probed with anti-caspase-3, then stripped and reprobed with anti-β-actin. Intact protein (solid arrow) and BP (open arrow) are indicated.
A–C. The density of the bands corresponding to each protein was evaluated by densitometric analysis. Densitometry units (U) were calculated relative to β-actin and values for the densitometric analyses obtained from four independent experiments. $^{*}P < 0.01$ GBS-infected treated MΦ versus GBS-infected non-treated MΦ.

that GBS-III-COH31 could cause gelsolin increase by β-haemolysin. Therefore, Western blot analysis, to investigate gelsolin increase, and propidium iodide (PI) uptake assay, to evaluate plasma membrane permeability alterations, were performed at 2 h in MΦ incubated, at an infection ratio of 1:100 with: (i) hiGBS-III-COH31, GBS-III-COH31 killed at 60°C for 30 min, a condition that causes GBS β-haemolysin inactivation; (ii) gGBS-III-COH31, GBS-III-COH31 grown for 18 h in the presence of 10 mg ml^{-1} glucose, a condition which abolishes GBS β-haemolysin synthesis; (iii) supernatant of GBS-III-COH31 growth in culture medium for 2 h; and (iv) GBS-III-COH31 in contiguous medium separated by a 0.45 μm pore size membrane of cell culture insert.

Under these conditions, we found no gelsolin increase (Fig. 9A) or alterations in MΦ plasma membrane permeability (Fig. 9B), which are both induced only by β-haemolytic GBS-III-COH31 (Fig. 9A and B). In fact, as shown in Fig. 9B, the MΦ infected with β-haemolytic GBS-III-COH31 showed 78% PI+ cells, while in the MΦ infected in all other conditions the percentage of PI+ cells was 18–21% similar to control MΦ (19%) (Fig. 9B). In spite of 78% PI+ cells the total number of MΦ infected with β-haemolytic GBS-III-COH31 at 2 h after infection, evaluated by Trypan blue exclusion assay, was the same as control MΦ and MΦ infected under all other conditions (results not shown).

To provide further evidence on the role of β-haemolysin in gelsolin increase, since it has been reported that some phospholipids such as dipalmitoylphosphatidylcholine

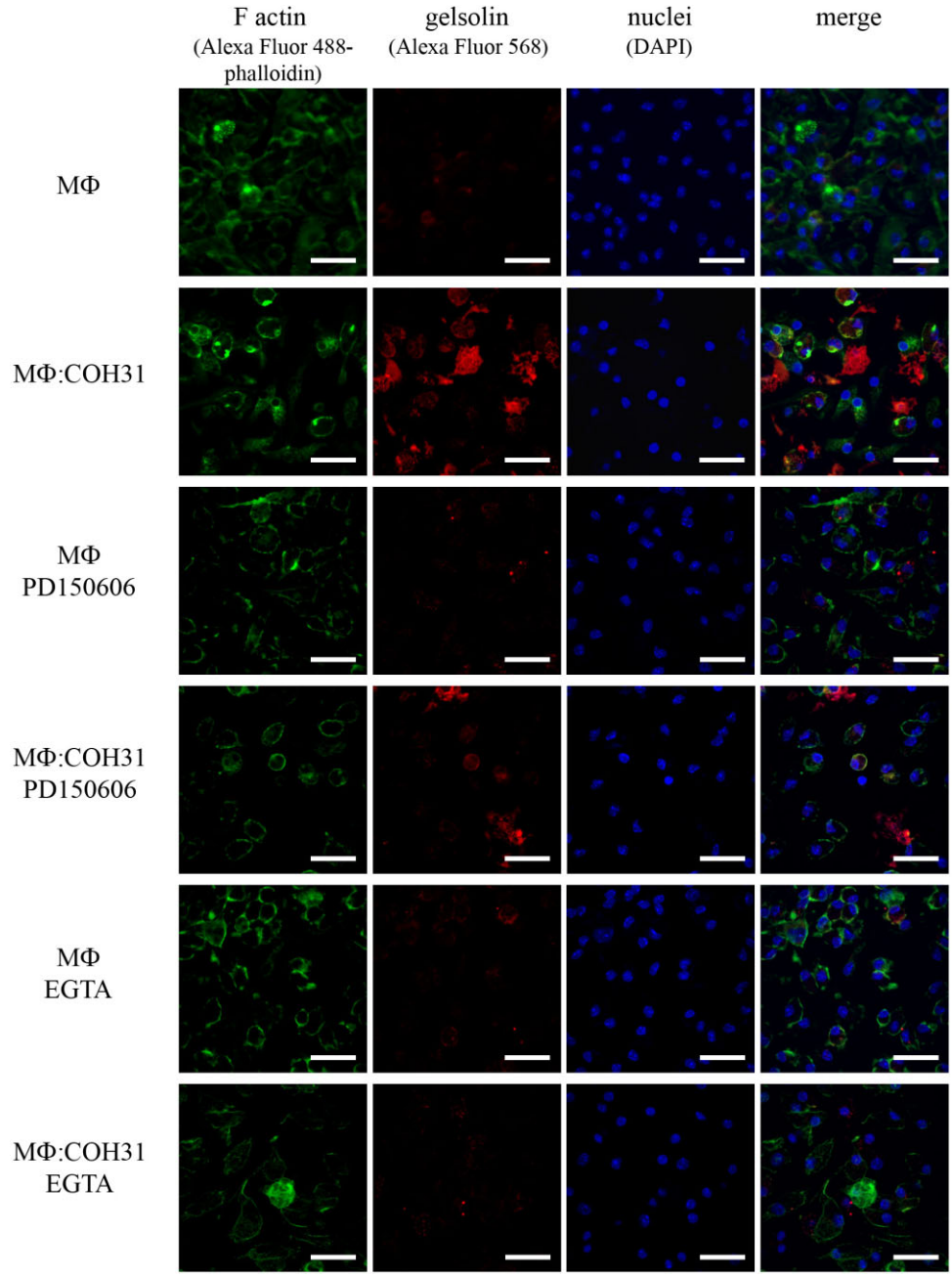

Fig. 8. Confocal microscope analysis of gelsolin expression in GBS-III-COH31-infected MΦ and effect of EGTA and PD150606.
Control MΦ (MΦ) and MΦ infected with GBS-III-COH31 (MΦ : COH31) at 1:100 ratio for 2 h, untreated or pretreated for 1 h with PD150606 (100 μM) and untreated or treated with EGTA (1 mM), were triple-labelled using Alexa Fluor 488 phalloidin to detect F-actin (green), an Alexa Fluor 568-labelled goat anti-mouse secondary Ab to detect gelsolin (red), and DAPI to visualized nuclei (blue), and observed by confocal microscopy. Bar, 50 μm (for all images).

(DPPC) inhibited GBS β-haemolytic activity (Fettucciari *et al.*, 2000; Nizet, 2002), we also analysed the effect of DPPC. We found that DPPC in MΦ infected with GBS-III-COH31 at a 1:100 ratio strongly inhibited gelsolin increase (Fig. 9A) and prevented alterations in membrane permeability (Fig. 9B).

Loss of β-haemolysin synthesis, due to growing GBS-III-COH31 in the presence of glucose, and inhibition of GBS β-haemolytic activity by heat-inactivation of GBS-III-COH31 or by DPPC, was confirmed by evaluating the β-haemolytic activity of gGBS-III-COH31, hiGBS-III-COH31 and GBS-III-COH31 in the presence or not of

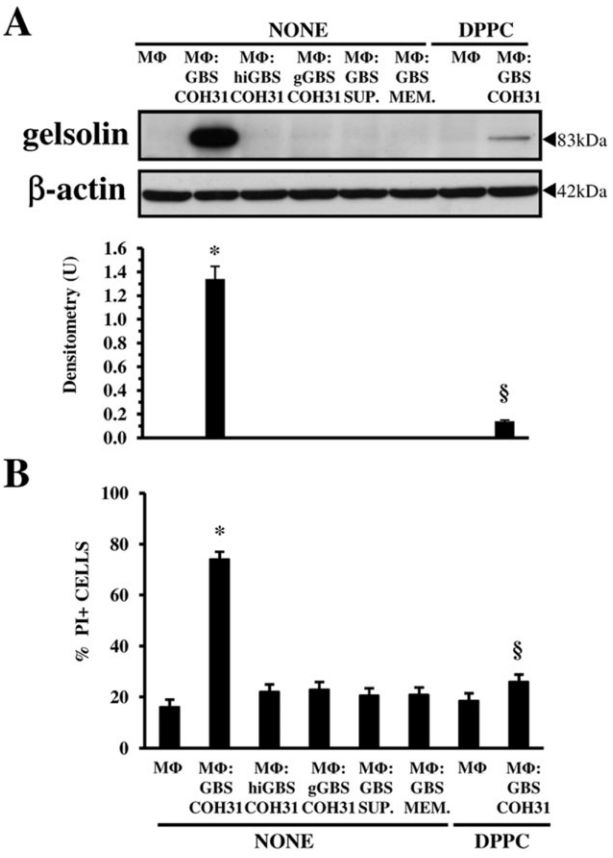

Fig. 9. Effect of β-haemolysin on gelsolin increase.
Control MΦ, MΦ infected with GBS-III-COH31 (MΦ : GBS-COH31) at a 1:100 ratio, MΦ infected with hiGBS-III-COH31 (MΦ : hiGBS-COH31) at a 1:100 ratio, MΦ infected with gGBS-III-COH31 (MΦ : gGBS-COH31) at a 1:100 ratio, MΦ incubated with supernatant of GBS-III-COH31 (MΦ : GBS-SUP.) growth in culture medium for 2 h at a concentration equivalent to that of MΦ : GBS ratio of 1:100, MΦ infected with GBS-III-COH31 at a 1:100 ratio, in contiguous medium separated by a 0.45 μm pore membrane of cell culture insert (MΦ : GBS-MEM.), MΦ treated with 2 mg ml^{-1} DPPC, MΦ infected with GBS-III-COH31 (MΦ : GBS-COH31) at a 1:100 ratio in the presence of 2 mg ml^{-1} DPPC, were recovered at 2 h infection, for cell lysate preparation, SDS-PAGE and Western blot analysis (A) or for PI uptake assay (B).
A. Western blot analysis. The filter was cut around 70 kDa and the top probed with anti-gelsolin and the bottom with anti-β-actin. The density of the bands corresponding to gelsolin was evaluated by densitometric analysis. Densitometry units (U) were calculated relative to β-actin and values for the densitometric analyses obtained from four independent experiments. $^{*}P < 0.01$ GBS-infected MΦ versus control MΦ; $^{§}P < 0.01$ GBS-infected treated MΦ versus GBS-infected non-treated MΦ.
B. PI uptake assay. Percentage of PI+ cells was determined evaluating PI uptake at flow cytometry. The data are means ± SD of six experiments performed in triplicate. $^{*}P < 0.01$ GBS-infected MΦ versus control MΦ; $^{§}P < 0.01$ GBS-infected treated MΦ versus GBS-infected non-treated MΦ.

DPPC against Sheep Red Blood cells (results not shown) with the β-haemolytic activity assay (Marchlewicz and Duncan, 1980) performed as described previously (Fettucciari *et al*., 2000).

Overall, these results suggest that GBS β-haemolysin is involved in MΦ gelsolin increase inducing extracellular Ca^{2+} influx by MΦ plasma membrane permeability defects.

Effect of different GBS strains on gelsolin expression in MΦ

Recently, we demonstrated that highly β-haemolytic GBS type V strain NCTC10/84 (GBS-V-10/84) (Wilkinson, 1977; Liu *et al*., 2004) and β-haemolytic GBS type III strain NEM316 (GBS-III-NEM316) (Glaser *et al*., 2002; Tettelin *et al*., 2005), like GBS-III-COH31 but with lower MΦ : GBS ratios, induce marked alterations in MΦ plasma membrane permeability allowing Ca^{2+} influx and calpain activation (Fettucciari *et al*., 2011), while the weak β-haemolytic GBS type Ia strain A909 (GBS-Ia-A909) and GBS type Ib strain H36B (GBS-Ib-H36B) (Tettelin *et al*., 2005) do not (Fettucciari *et al*., 2011). Since as above reported β-haemolysin is involved in MΦ gelsolin increase induced by MΦ : GBS-III-COH31 interaction to determine if gelsolin increase in MΦ is a general MΦ response to more β-haemolytic GBS or is specific for the clinical β-haemolytic GBS strain COH31 used in this study we employed the clinically isolated highly β-haemolytic GBS-V-10/84 (Wilkinson, 1977; Liu *et al*., 2004), the clinically isolated and fully sequenced β-haemolytic GBS-III-NEM316 (Glaser *et al*., 2002; Tettelin *et al*., 2005), and the clinically isolated and fully sequenced weakly β-haemolytic GBS-Ia-A909 and GBS-Ib-H36B (Tettelin *et al*., 2005) for which a different β-haemolytic activity has been demonstrated (Marchlewicz and Duncan, 1980; Nizet *et al*., 1996; Liu *et al*., 2004) and a different: serotype, multilocus sequence type (ST) and dispensable genome (Glaser *et al*., 2002; Tettelin *et al*., 2005; Brochet *et al*., 2006). Therefore, Western blot analysis to examine the gelsolin increase and PI uptake assay to evaluate plasma membrane permeability alterations, were performed in MΦ infected with GBS-III-NEM316, GBS-V-10/84, GBS-Ia-A909, GBS-Ib-H36B, at different MΦ : GBS ratios for 2 h (time at which we observed the maximum gelsolin increase by GBS-III-COH31).

The interaction of MΦ both with GBS-III-NEM316 and GBS-V-10/84 induced at 2 h after infection in a ratio-dependent manner a strong gelsolin increase as shown by Western blot analysis (Fig. 10A) and marked alterations in MΦ plasma membrane permeability, as shown by PI uptake assay which found about 78% MΦ PI+ with GBS-III-NEM316 at a ratio of 1:20 and 72% MΦ PI+ with GBS-V-10/84 at a ratio of 1:20 (Fig. 10B). In contrast, GBS-Ia-A909 and GBS-Ib-H36B did not induce gelsolin also at the highest MΦ : GBS ratio of 1:100 (Fig. 10A) and in MΦ infected with GBS-Ia-A909 and GBS-Ib-H36B only a weak increase in the percentage of PI+ cells was found (Fig. 10B).

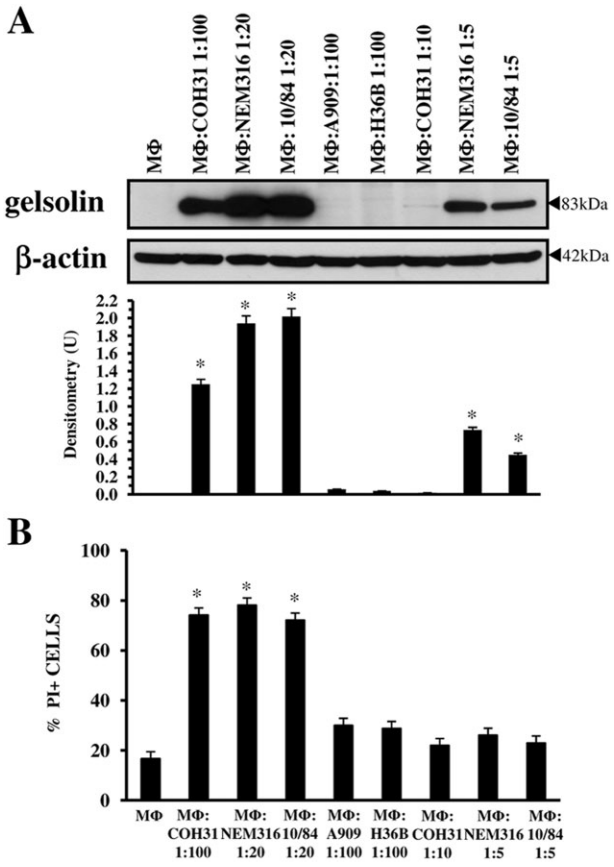

Fig. 10. Effect of different GBS strains on gelsolin expression in MΦ.
Control MΦ, MΦ infected with GBS-III-COH31 (MΦ : COH31), MΦ infected with GBS-III-NEM316 (MΦ : NEM316), MΦ infected with GBS-V-10/84 (MΦ:10/84), MΦ infected with GBS-Ia-A909 (MΦ : A909) and MΦ infected with GBS-Ib-H36B (MΦ : H36B) at the indicated ratios, were recovered at 2 h after infection for cell lysate preparation, SDS-PAGE and Western blot analysis (A) or for PI uptake assay (B).
A. Western blot analysis. The filter was cut around 70 kDa, the top probed with anti-gelsolin, the bottom with anti-β-actin. The density of the bands corresponding to gelsolin was evaluated by densitometric analysis. Densitometry units (U) were calculated relative to β-actin and values for the densitometric analyses obtained from four independent experiments. $*P < 0.01$ GBS-infected MΦ versus control MΦ.
B. PI uptake assay. The percentage of PI+ cells was determined evaluating PI uptake at flow cytometry. The data are means ± SD of six experiments performed in triplicate. $*P < 0.01$ GBS-infected MΦ versus control MΦ.

The above results demonstrating that marked increase of gelsolin in MΦ is induced by the interaction of MΦ with GBS-III-NEM316 and with GBS-V-10/84 that have a β-haemolytic titre of 8 and 64 respectively, but not with GBS-Ia-A909 or GBS-Ib-H36B that have a β-haemolytic titre of 4 (Marchlewicz and Duncan, 1980; Nizet *et al.*, 1996; Liu *et al.*, 2004), indicate that only highly β-haemolytic GBS induced gelsolin increase in MΦ.

Altogether these data indicate that, like GBS-III-COH31, a marked increase in gelsolin levels in MΦ is also induced by interaction of MΦ with other highly β-haemolytic GBS strains, confirming that β-haemolytic activity is directly involved in gelsolin increase.

Gelsolin increase and MΦ apoptosis

In agreement with the results of our previous studies, GBS-III-COH31 induces MΦ apoptosis at 24 h in an infection-ratio-dependent manner (Fettucciari *et al.*, 2000; 2006; Fig. S1). Since it is well known that gelsolin is intimately associated with pro-apoptotic or anti-apoptotic functions (Kothakota *et al.*, 1997; Kwiatkowski, 1999; Koya *et al.*, 2000; Kusano *et al.*, 2000; Silacci *et al.*, 2004; Li *et al.*, 2012), we investigated first if the gelsolin increase was caused by MΦ apoptosis induction by other inducers and then its role in GBS-induced apoptosis.

For the first aim we used two different inducers of apoptosis in MΦ, the CHX at 200 μg ml^{-1} (Gargalovic and Dory, 2003; Croons *et al.*, 2007; Donovan *et al.*, 2009) and the STS at 5 μM (Rabkin and Kong, 2002; Benjamins *et al.*, 2003; Norberg *et al.*, 2008). To compare the effect of these apoptotic stimuli with the effect of GBS, gelsolin was analysed by Western blot in lysates of MΦ treated for 2 h, with CHX (200 μg ml^{-1}) or with STS (5 μM), and MΦ apoptosis was evaluated at 2 and 24 h measuring the percentage of apoptotic MΦ at flow cytometry, by assessment of DNA content after staining with PI in MΦ treated for 2 or 24 h with 200 μg ml^{-1} CHX or with 5 μM STS.

Western blot analysis showed that gelsolin did not increase in MΦ at 2 h after addition of the apoptotic stimuli STS and CHX (Fig. 11A) although at 24 h respectively about 85% of apoptosis in MΦ treated with 5 μM STS for 24 h and 45% apoptosis in MΦ treated with 200 μg ml^{-1} CHX for 24 h was found (Fig. 11B).

For the second aim, to evaluate the possible functional role of gelsolin increase in GBS-induced MΦ apoptosis, we used the gelsolin small interfering RNA (siRNA) mediated gene silencing technique (Fettucciari *et al.*, 2006) to knockdown gelsolin. For this, MΦ were transfected with 100 nM siRNA specific for gelsolin. At 72 h post transfection the cells were harvested for mRNA expression analysis by qRT-PCR or infected with GBS-III-COH31 for analysis of apoptosis. In these experiments to better assess the role of gelsolin in MΦ apoptosis by GBS, we used three MΦ : GBS infection ratios that showed ratio-dependent effects (see Fig. S1). We found that transfection of MΦ with gelsolin siRNA resulted in about 76% decrease of mRNA level of gelsolin compared to non-transfected MΦ (Fig. 12A). Mock transfection and transfection with 100 nM control non-targeting siRNA in MΦ did not affect mRNA expression of gelsolin (Fig. 12A). As shown in Fig. 12B,

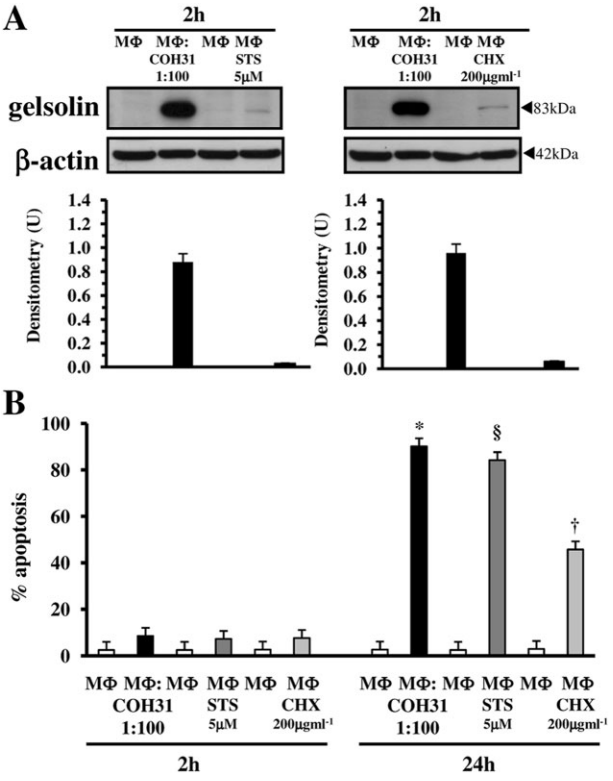

Fig. 11. Effect of two different MΦ apoptotic stimuli on gelsolin increase and apoptosis.
A. Effect of STS and CHX on gelsolin expression by Western blot analysis. Lysates from control MΦ and lysates from MΦ infected with GBS-III-COH31 (MΦ : COH31) at a 1:100 ratio prepared at 2 h after infection, lysates from control MΦ and lysates from MΦ treated with STS (5 μM; MΦ : STS) or with CHX (200 μg ml^{-1}; MΦ : CHX) prepared at 2 h after stimulation, were subjected to SDS-PAGE. The filters were cut around 70 kDa and the top sections probed with anti-gelsolin, while the bottom sections were probed with anti-β-actin. The density of the bands corresponding to gelsolin was evaluated by densitometric analysis. Densitometry units (U) were calculated relative to β-actin and values for the densitometric analyses obtained from four independent experiments.
B. Analysis of induction of MΦ apoptosis by STS and CHX at flow cytometry. Apoptosis of control MΦ, MΦ infected with GBS-III-COH31 at a 1:100 ratio, MΦ treated with STS (5 μM; MΦ : STS), MΦ treated with CHX (200 μg ml^{-1}; MΦ : CHX) was measured at 2 and 24 h evaluating by flow cytometry the percentage of hypodiploid nuclei. Data are means ± SD of six experiments done in triplicate. $^{*}P < 0.01$ GBS-infected MΦ versus control MΦ. $^{§}P < 0.01$ STS-treated MΦ versus control MΦ. $^{†}P < 0.01$ CHX-treated MΦ versus control MΦ.

downregulation of gelsolin expression resulted in about 17% increase of GBS-induced MΦ apoptosis at an infection ratio of 1:100, in about 35% increase of GBS-induced MΦ apoptosis at an infection ratio of 1:50 and in about 55% increase of GBS-induced MΦ apoptosis at a infection ratio of 1:10. Transfection with 100 nM control non-targeting siRNA in MΦ did not affect GBS-induced MΦ apoptosis (Fig. 12B).

Altogether these data indicate that gelsolin increase is not induced by any apoptotic stimuli and in our infection model contributes to counter the MΦ apoptosis induced by GBS.

Discussion

This study shows for the first time that in the complex interaction of GBS with MΦ is also involved gelsolin. Here we demonstrate that the interaction of MΦ with β-haemolytic GBS-III-COH31, in a time- and infection-ratio-dependent manner, leads very early to a strong gelsolin increase in MΦ. In fact, at 0.5 h of infection with GBS-III-COH31, at a ratio of 1:100, there is a significant

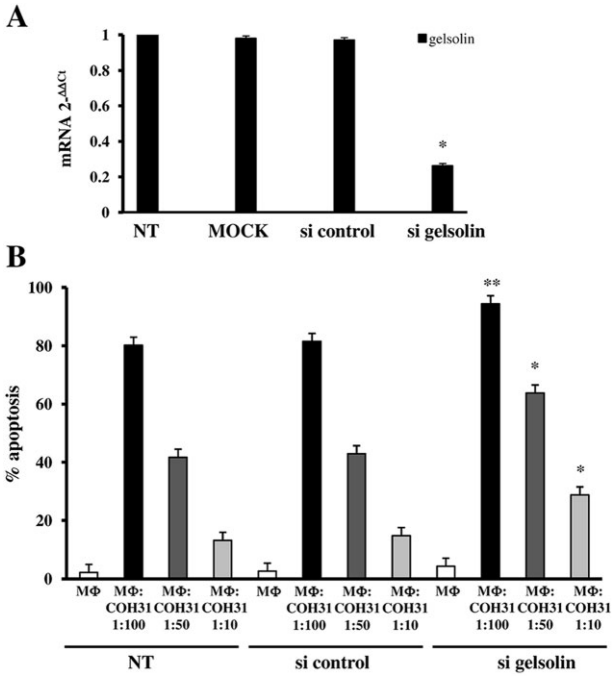

Fig. 12. Effect of gelsolin knockdown on GBS-III-COH31-induced MΦ apoptosis.
A. Analysis of gelsolin mRNA by qRT-PCR following silencing of gelsolin gene by siRNA. At 72 h post transfection, cDNA from MΦ transfected, with vehicle alone (MOCK), control non-targeting siRNA (100 nM; si control), gelsolin (100 nM; si gelsolin) or non-transfected (NT), were subjected to qRT-PCR and data expressed as $2^{-\Delta\Delta Ct}$. $^{*}P < 0.01$ MΦ transfected with siRNA versus non-transfected MΦ.
B. Effect of gelsolin silencing on apoptosis. At 72 h post transfection, MΦ transfected with control non-targeting siRNA (100 nM; si control), gelsolin siRNA (100 nM; si gelsolin) or non-transfected (NT), infected or not with GBS-III-COH31 at 1:100, 1:50 and 1:10 ratios for 2 h, were recovered at 24 h and apoptosis measured evaluating the percentage of hypodiploid nuclei at flow cytometry. Data are means ± SD of four experiments done in triplicate. $^{*}P < 0.01$ GBS-infected MΦ transfected with siRNA for gelsolin versus non-transfected GBS infected MΦ; $^{**}P < 0.05$ GBS-infected MΦ at 1:100 ratio transfected with siRNA for gelsolin versus non-transfected GBS-infected MΦ at 1:100 ratio.

increase of gelsolin that continues to increase up to 2 h of infection, time at which GBS induced the maximum MΦ plasma membrane permeability defects, as demonstrated in this study and previously (Fettucciari *et al*., 2000; 2006; 2011), and the maximum intracellular Ca^{2+} increase (Fettucciari *et al*., 2000; 2006). While we observed no gelsolin expression, at all times examined, with GBS-III-COH31 at a MΦ : GBS infection ratio of 1:10 which did not induce plasma membrane permeability defects.

Since it is well known that protein level increase in the cells could be due to transcriptional events, translation events, alterations of protein turnover by proteasome inhibition or by activation of protein-kinases (Ciechanover, 1998; Nandi *et al*., 2006; Ji *et al*., 2010), we investigated which of these mechanisms was involved in the gelsolin increase induced by MΦ : GBS-III-COH31 interaction. Our results show that: (i) gelsolin mRNA did not increase after GBS-III-COH31 infection of MΦ; (ii) CHX, an inhibitor of protein synthesis (Fettucciari *et al*., 2000; Croons *et al*., 2007; Ji *et al*., 2010) at a concentration of 50 $\mu g\ ml^{-1}$, did not inhibit the increase of gelsolin protein levels; (iii) proteasome is not involved in gelsolin increase, because GBS-III-COH31 did not inhibit proteasome activity, as demonstrated by no accumulation of multiubiquitinylated proteins, and proteasome inhibitors alone or with simultaneous CHX treatment did not increase gelsolin stability, (iv) gelsolin increase is not due to translocation of gelsolin from a different compartment or structure, as showed by analysis of gelsolin expression on subcellular fractions, (v) the STS, a potent and broad spectrum inhibitor of a variety of protein-kinases (Toledo and Lydon, 1997; Ji *et al*., 2010), did not significantly inhibit gelsolin increase, (vi) gelsolin seems a long-living protein. Indeed by CHX inhibition experiments (Zhou, 2004), we were unable to determine gelsolin $t_{1/2}$ as we found a similar level of gelsolin in CHX-treated GBS-infected MΦ and non-treated GBS-infected MΦ at all times examined. Therefore, the gelsolin increase in MΦ after GBS infection is independent of transcription, de novo protein synthesis, proteasome function and protein-kinases activation.

However, in the light of the above results, since it is known that gelsolin is a Ca^{2+}-regulated molecule which at low [Ca^{2+}] has a compact, globular, inactive structure while at increasing [Ca^{2+}] it opens up (Kwiatkowski, 1999; Kiselar *et al*., 2003; McGough *et al*., 2003; Silacci *et al*., 2004; Ashish *et al*., 2007; Li *et al*., 2012), the gelsolin increase in our model could be due to Ca^{2+} and also to proteolytic control by some cellular proteases. In fact, it is known that, although the ubiquitin proteasome pathway constitutes the bulk of regulated cytoplasmic proteolysis, in most cases other cellular protease apparatuses play significant roles in post-translational regulation of cellular proteins levels (Coux *et al*., 1996; Carafoli and Molinari, 1998; Ciechanover, 1998; Pillay *et al*., 2002; Goll *et al*., 2003; Zhou, 2004; Nandi *et al*., 2006; Bhatia *et al*., 2013).

Therefore in an attempt to define the mechanism involved in gelsolin increase, we first investigated the role of Ca^{2+} in MΦ gelsolin increase, since we previously showed that GBS causes a progressive and massive influx of extracellular Ca^{2+} by inducing MΦ plasma membrane permeability defects (Fettucciari *et al*., 2000; 2006). In agreement with that observed in other experimental models which showed gelsolin upregulation by Ca^{2+} (Silacci *et al*., 2004; Ji *et al*., 2010; Li *et al*., 2012), the GBS-III-COH31-induced gelsolin increase was mediated by extracellular Ca^{2+} influx in MΦ. In fact, EGTA, a chelator of extracellular Ca^{2+}, prevents the gelsolin increase induced by MΦ : GBS interaction and the addition of an excess of $CaCl_2$ but not $MgCl_2$ during incubation with EGTA reverses the effect of EGTA. Furthermore BAPTA/AM, an intracellular Ca^{2+} chelator, did not prevent gelsolin increase. Therefore influx of extracellular Ca^{2+}, without the emptying of intracellular Ca^{2+} stores, is the principal responsible for gelsolin increase and represents the first step in the molecular mechanism involved in gelsolin increase.

Subsequently, we also investigated if the other cellular apparatuses, such as calpains, lysosomes and caspases that play significant roles in protein turnover (Coux *et al*., 1996; Carafoli and Molinari, 1998; Ciechanover, 1998; Pillay *et al*., 2002; Goll *et al*., 2003; Zhou, 2004; Nandi *et al*., 2006; Bhatia *et al*., 2013) are involved in the MΦ gelsolin increase by GBS.

Since we have previously demonstrated that GBS-III-COH31, as a result of the influx of Ca^{2+}, activates the Ca^{2+}-dependent protease calpains in MΦ (Fettucciari *et al*., 2006; 2011), we first determined if the gelsolin increase was influenced by calpain activation. The PD150606, a calpain inhibitor (Wang *et al*., 1996; Carafoli and Molinari, 1998; Goll *et al*., 2003; Fettucciari *et al*., 2006), strongly reduced the gelsolin increase, thus indicating that the gelsolin increase in MΦ is also regulated by calpains and this represents the second step of the molecular mechanism involved in gelsolin increase.

Instead, no inhibition or increase of gelsolin was observed with the cathepsin inhibitors, CA-074 Me, NH_4Cl and Pepstatin A, indicating that lysosomal cathepsins are not involved in gelsolin increase.

Post-translation regulation of several proteins involves altered degradation by caspases (Zhou, 2004; Bhatia *et al*., 2013). It is well known that caspase-3 cleaves gelsolin (Kothakota *et al*., 1997; Jänicke *et al*., 1998; Kwiatkowski, 1999; Azuma *et al*., 2000; Koya *et al*., 2000; Silacci *et al*., 2004; Li *et al*., 2012). Since we have demonstrated that GBS-III-COH31, as a result of calpain activation degrades caspase-3 (Fettucciari *et al*., 2006;

Fig. 7), gelsolin increase in GBS-infected MΦ may also be due to post-translational regulation based on reduced degradation of gelsolin owing to caspases degradation. We then investigated if caspases are involved in gelsolin increases. We found that caspase inhibition by the caspase inhibitor BAF enhanced gelsolin increase induced by GBS-III-COH31 in MΦ. These results together with the demonstration that calpain inhibition, which prevents caspase cleavage, reduced gelsolin increase, suggest that lack of gelsolin degradation by caspase-3 contributes to gelsolin overexpression in GBS-infected MΦ.

To define the GBS-III-COH31 triggering event involved in MΦ gelsolin increase we tested the role of GBS β-haemolysin. GBS β-haemolysin contributes to GBS pathogenicity by different actions against various targets including its activity, like pore-forming proteins, against the membrane of several eukaryotic cells (Nizet *et al*., 1996; Nizet, 2002; Liu *et al*., 2004; Hensler *et al*., 2008; Maisey *et al*., 2008; Rajagopal, 2009) that in MΦ lead to plasma membrane permeability defects which allow a massive Ca^{2+} influx (Fettucciari *et al*., 2000; 2006; 2011). The crucial role of β-haemolysin in GBS pathogenicity is also supported by the observation that the virulence of haemolysin-deficient GBS mutants is attenuated in various animal models of GBS infection and that non β-haemolytic strains rarely cause infections (Liu *et al*., 2004; Sigge *et al*., 2008; Rajagopal, 2009). Our data show that the expression of GBS β-haemolytic activity is directly correlated with gelsolin increase. In fact, the gelsolin increase in MΦ was not induced under conditions that prevent/inactivate β-haemolytic activity of GBS-III-COH31 such as: infection with gGBS-III-COH31, incubation with hiGBS-III-COH31, incubation with the culture supernatant of GBS-III-COH31, incubation with GBS-III-COH31 in contiguous medium separated by a membrane with 0.45 μm pores, infection with GBS-III-COH31 β-haemolytic in the presence of DPPC, a phospholipid that inhibits β-haemolysin. Moreover, the demonstration that in these conditions the alterations of plasma membrane permeability did not occur indicates that GBS β-haemolysin generating small pores alters the MΦ plasma membrane so allowing the influx of Ca^{2+} and consequent calpain activation, which are both responsible for gelsolin increase. Furthermore, highly β-haemolytic GBS-III-NEM316 and GBS-V-10/84 which cause MΦ plasma membrane permeability alterations, like GBS-III-COH31, induced a strong gelsolin increase in MΦ, while the weakly β-haemolytic GBS-Ia-A909 and GBS-Ib-H36B, which do not cause significant MΦ plasma membrane permeability alterations, did not induce MΦ gelsolin increase, so correlating MΦ gelsolin response with the level of β-haemolytic activity of GBS strains.

We previously demonstrated that GBS by β-haemolysin induces MΦ cytoskeletal disruption and then apoptosis. A regards correlation between these two effects preliminary results showing that GBS-induced apoptosis occurs also in the absence/reduction of MΦ cytoskeletal disruption suggest that MΦ cytoskeletal disruption and apoptosis are two independent phenomena linked only by the necessity of Ca^{2+} influx and calpain activation (K. Fettucciari *et al*., unpubl. obs.). A regards correlation of gelsolin increase with MΦ cytoskeletal disruption and apoptosis, it is very interesting that the gelsolin level was already increased at 0.5 h, the time frame at which neither alteration of cytoskeletal protein expression or activation of pro-apoptotic signal transduction were found, ruling out that gelsolin increase is due to these processes. As a further confirmation that gelsolin increase is not due to apoptosis no early gelsolin increase was observed during induction of MΦ apoptosis with two different apoptotic stimuli, the STS and CHX (Rabkin and Kong, 2002; Benjamins *et al*., 2003; Gargalovic and Dory, 2003; Croons *et al*., 2007; Norberg *et al*., 2008; Donovan *et al*., 2009).

It is known that gelsolin has pleiotropic effects on the F-actin, since the severing, uncapping and binding of actin filaments by gelsolin enhances the number of filaments and provides many free ends for polymerization (Kwiatkowski, 1999; McGough *et al*., 2003; Silacci *et al*., 2004; Li *et al*., 2012). Since we previously showed that during GBS-infection of MΦ the expression levels of β-actin are not affected while the expression levels of several focal adhesion proteins, actin binding proteins and microtubule proteins are strongly decreased (Fettucciari *et al*., 2011), the early gelsolin increase induced by MΦ : GBS-III-COH31 interaction, leads to the hypothesize that gelsolin could bind to actin and so protect the actin by calpain cleavage. Therefore, gelsolin could also be a MΦ attempt to maintain the integrity and expression levels of actin during GBS infection. However in the light of: (i) the role of gelsolin in increasing both the amounts of filamentous actin and actin polymerization; (ii) the knowledge that gelsolin null neutrophils and fibroblasts have a deficit in the early stages of phagocytosis (May and Machesky, 2001; Silacci *et al*., 2004; Groves *et al*., 2008; Melendez and Tay, 2008; Li *et al*., 2012); and (iii) the knowledge that pathogens interfere with gelsolin function to invade mammalian cells (May and Machesky, 2001; Cossart, 2004; Cossart and Sansonetti, 2004; McGhie *et al*., 2004; Silacci *et al*., 2004; Groves *et al*., 2008; Melendez and Tay, 2008; Li *et al*., 2012), the gelsolin increase in MΦ could be an early MΦ response activated by Ca^{2+} influx and calpain activation in an attempt to enhance GBS uptake and maintain dynamic/functionality of the actin cytoskeleton during progressive disruption of the MΦ cytoskeleton by GBS.

Since it is known that gelsolin can also play pro- or anti-apoptotic effects (Kothakota *et al.*, 1997; Kwiatkowski, 1999; Koya *et al.*, 2000; Kusano *et al.*, 2000; Silacci *et al.*, 2004; Li *et al.*, 2012), we knockdowned gelsolin expression in MΦ with siRNA specific for gelsolin and evaluated the effect on induction of MΦ apoptosis. Gelsolin knockdown makes MΦ more susceptible to apoptosis induction by GBS suggesting that gelsolin increase contributes also in counteracting GBS-induced MΦ apoptosis so acting in our model as an anti-apoptotic.

In conclusion, this study demonstrates for the first time that an early MΦ response to the β-haemolytic strains of GBS (GBS-III-COH31, GBS-III-NEM316 and GBS-V-10/84) is a marked early gelsolin increase, mediated by an influx of extracellular Ca^{2+}, calpain activation and consequent caspase-3 degradation without involvement of transcriptional and translation events or protein turnover alterations (Fig. 13). The response is highly dependent on the expression level of β-haemolytic activity and plays an anti-apoptotic role but also appears to contribute to controlling phagocytosis and cytoskeleton dynamics in the early phase of infection (Fig. 13). However, further studies are necessary to better and completely define the role of gelsolin in GBS infection and to understand whether gelsolin could be a part of the natural immune response against GBS.

Experimental procedures

Reagents

PD150606 (a selective inhibitor for μ- and m-calpain directed to the Ca^{2+} binding sites IC50: 210 nM for μ-calpain; IC50: 370 nM for m-calpain), CA-074 Me (an inhibitor of cathepsin B; IC50: 2.24 nM), Pepstatin A (an inhibitor of cathepsin D; IC50: 10 nM), NH_4Cl (an inhibitor of all lysosomal proteases; IC50: 5 mM), BAF (a broad-spectrum caspase inhibitor; IC50: 1.2 nM), *clasto*-Lactacystin (a proteasome inhibitor; IC50: 1 μM), MG132 (a proteasome inhibitor; IC50: 0.1 μM), BAPTA/AM (a intracellular Ca^{2+} chelator; IC50: 1.3 μM), were obtained from Calbiochem (San Diego, CA). STS (a protein-kinase inhibitor; maximum IC50: 20 nM), CHX (a de novo synthesis inhibitor), BSA, Triton X-100, DPPC (an inhibitor of β-haemolytic activity), PI, mouse monoclonal Abs anti-β-actin (clone AC-15), anti-β-Tubulin (clone TUB 2.1), anti-Talin (clone 8D4), anti-Vinculin (clone hVIN-1), were obtained from Sigma (St Louis, MO). Mouse Ab anti-gelsolin (clone 2) was obtained from BD Transduction Laboratories (Lexington, KY). Mouse α-spectrin (nonerythroid; MAB1622) mAb was purchased from Chemicon International (Temecula, CA). Mouse anti-ubiquitinylated proteins mAb was obtained from Biomol International L.P. (Plymouth Meeting, PA). Rabbit polyclonal Ab anti-MnSOD was obtained from Upstate Biotechnology (Lake placid, NY). Horseradish Peroxidase (HRP)-conjugated secondary anti-mouse IgG and ECL system were obtained from GE Healthcare (Little Chalfont Buckinghamshire, UK), HRP-linked secondary anti-rabbit IgG and rabbit polyclonal Ab anti-caspase-3 were obtained from Cell Signaling Technology. 4′,6′-diamidino-2-phenylindole,dilactate (DAPI), ProLong Gold antifade reagent, Alexa Fluor 568-labelled goat anti-mouse IgG (H + L) Ab, and Alexa Fluor 488 phalloidin were obtained from Molecular Probes, Invitrogen detection technologies (Eugene, Oregon). Paraformaldehyde extra pure was obtained from Merck (Darmstadt, Germany). The siRNA duplexes specific for mouse gelsolin (ON-TARGETplus Catalogue No. L-057211) and non-targeting (ON-TARGETplus Catalogue No. D001810) were obtained from Dharmacon RNA Technologies (Boulder, CO). The siRNA for gelsolin, contained four RNA sequences in a pool SmartPool selected from the NCBI RefSeq Database by a proprietary algorithm.

Microorganisms

GBS, type III, strain COH31 r/s (GBS-III-COH31), clinically isolated from a foot ulcer of a diabetic adult, rendered resistant to rifampicin and streptomycin (Gibson *et al.*, 1989) was kindly provided by Dr. M. Wessel (Channing Laboratory, Boston, MA). GBS-III-COH31 was grown in Todd Hewitt Broth (THB; Difco Laboratories, Detroit, MI) at 37°C and aliquots stored at −70°C until used.

GBS, type V, strain NCTC10/84 (*Streptococcus agalactiae* ATCC®49447) (GBS-V-10/84) purchased from American Type Culture Collection (Manassas, USA) (Wilkinson, 1977; Nizet *et al.*, 1996; Liu *et al.*, 2004), GBS, type III, strain NEM316 (GBS-III-NEM316; CIP 82.45), GBS, type Ia strain A909 (GBS-Ia-A909; CIP 82.43), and GBS, type Ib strain H36B (GBS-Ib-H36B; CIP 82.42) purchased from the Collection of the Institute Pasteur (Paris, France) (Glaser *et al.*, 2002; Liu *et al.*, 2004; Tettelin *et al.*, 2005; Brochet *et al.*, 2006), were propagated according to their respective product information sheets, then aliquots were stored at −70°C until used.

For assays, all the GBS strains were grown in THB overnight, back diluted in fresh THB and grown to late-log phase, washed three times with PBS (3000 *g*, 10 min, 22°C) and resuspended in RPMI-1640 with glutamine to the desired number of cfu ml^{-1} (Cornacchione *et al.*, 1998). Bacterial numbers were determined photometrically (600 nm) and confirmed in each experiment by quantitative culture on Islam agar (Difco Laboratories) plates containing 5% heat-inactivated horse serum (Cornacchione *et al.*, 1998) and on Todd Hewitt agar (THA, Difco Laboratories).

For some experiments, GBS-III-COH31, resuspended to the desired number of cfu ml^{-1} as described above (Cornacchione *et al.*, 1998), was heat-inactivated (0.5 h 60°C; hiGBS-III-COH31) then extensively washed in PBS (3000 *g*, 10 min, 22°C), aliquoted and stored at −70°C until used. Sterility was confirmed by culture on THA plates.

For some experiments GBS-III-COH31 was grown for 18 h in THB in the presence of 10 mg ml^{-1} glucose (gGBS-III-COH31) conditions which do not allow β-haemolytic activity expression (Fettucciari *et al.*, 2000; 2011; Nizet, 2002), and then treated as described above.

For experiments with GBS-III-COH31 supernatant, GBS-III-COH31 was grown for 2 h in RPMI-1640 medium with 10% FBS at a concentration equivalent to the 1:100 MΦ : GBS ratio (3×10^8 cfu of GBS-III-COH31 for each 2 ml medium). The bacteria were then pelleted by centrifugation at 3000 *g* for 10 min at 22°C and the resulting supernatant was filter sterilized with a 0.2 μm nitrocellulose membrane.

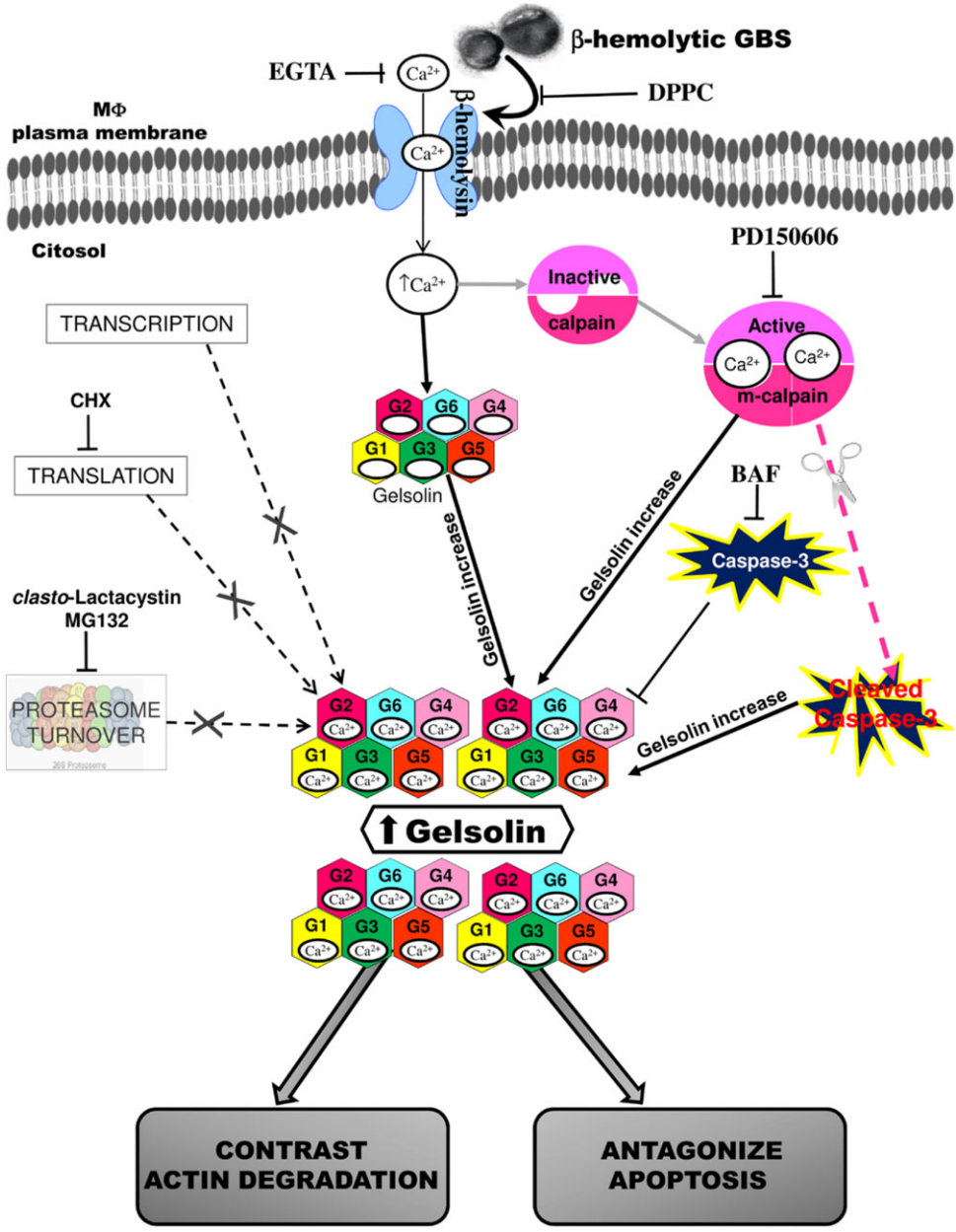

Fig. 13. Schematic diagram of the mechanisms of MΦ gelsolin increase in response to GBS.
GBS by β-haemolysin induces MΦ plasma membrane permeability alterations allowing progressive and massive extracellular Ca^{2+} influx that leads to gelsolin increase by: (1) direct effect; (2) activation of calpain; (3) calpains mediated caspase-3 degradation. In fact, DPPC (an inhibitor of β-haemolytic activity), EGTA (an extracellular Ca^{2+} chelator) and PD150606 (a calpain inhibitor) inhibit gelsolin increase. The role of caspase-3 was confirmed by the caspase inhibitor BAF which enhances gelsolin increase (filled lines). Gelsolin increase is independent by: (i) transcription, no increase of mRNA for gelsolin was found by qRT-PCR, (ii) translational, CHX, an inhibitor of protein synthesis, not affected gelsolin increase, (iii) proteasome turnover, *clasto*-Lactacystin and MG132 (proteasome inhibitors), not affected gelsolin increase.
MΦ gelsolin increase contrast apoptosis and attempt to maintain dynamic/functionality of actin cytoskeleton during progressive disruption of MΦ cytoskeleton by GBS.
Gelsolin is represent with it six domain (designated as G1-G6) each contains one Ca^{2+} binding site. Black filled arrows indicated mechanisms involved in gelsolin increase. Black dashed arrows indicated mechanisms not involved in gelsolin increase. Gray filled arrow indicated Ca^{2+}-mediated calpain activation. Fuchsia dashed arrow indicated degradation of caspase by calpain.

Preparation of peritoneal MΦ

Outbred female CD-1 8- to 10-week old mice were obtained from Charles River Breeding Laboratories (Calco, Milan, Italy).

Murine peritoneal MΦ were elicited by intraperitoneal injection of 1 ml 10% Thioglycollate broth solution (Difco Laboratories) and cells were recovered 4 days later as previously described (Fettucciari *et al.*, 2000). Cells were resuspended in cold antibiotic-free RPMI-1640 medium with 10% FBS (complete medium) and cell viability evaluated by Trypan blue exclusion method.

The purity of Thioglycollate-elicited MΦ obtained by washing the peritoneal cavity was more than 80%, as determined by binding of monoclonal Ab to CD14 (Fettucciari *et al.*, 2006). When the MΦ were allowed to adhere for 90 min in 6-well tissue culture plates and the non-adherent cells removed by washing, the resulting MΦ population was 98% pure as determined by non-specific esterase staining and by binding of monoclonal Ab to CD14 (Fettucciari *et al.*, 2006).

For PI uptake assay and Trypan Blue exclusion assay, MΦ were harvested from monolayers by gently pipetting repeatedly after incubation with EDTA 0.5 mM in PBS without Ca^{2+} and Mg^{2+} pH 8 at 37°C for 15 min which rather than MΦ monolayer scraping, allows the recovery of MΦ without significantly altering plasma membrane permeability and cell viability.

Infection procedure

MΦ (3×10^6 in 2 ml complete medium) were allowed to adhere for 90 min at 37°C, 5% CO_2 in 6-well plates and then non-adherent cells were removed. After 18 h, MΦ monolayers were infected with GBS-III-COH31, at a cell : microorganism ratio of 1:100, 1:50 or 1:10 for 0.5 h, 1 h or 2 h. In some experiments we used MΦ, seeded 18 h before in a 6-well plate, infected for 2 h with GBS-III-COH31, at a cell : microorganism ratio of 1:100, washed and re-incubated for 3 h or 6 h in complete medium containing 100 U ml^{-1} penicillin and 100 μg ml^{-1} gentamicin. Control MΦ were incubated in medium without GBS-III-COH31 for the same times. For evaluation of apoptosis we used: (i) MΦ, seeded 18 h before in a 6-well plate, infected at different cell : microorganism ratio and times; and (ii) MΦ, seeded 18 h before in a 6-well plate, infected at the indicated cell : microorganism ratio for 2 h washed and re-incubated for 24 h in complete medium containing 100 U ml^{-1} penicillin and 100 μg ml^{-1} gentamicin. Control MΦ were incubated in medium without GBS-III-COH31 for the same times.

Infection of MΦ monolayers with hiGBS-III-COH31 or gGBS-III-COH31 at a cell : microorganism ratio of 1:100 was as described above. For some experiments MΦ monolayers were also incubated for 2 h with GBS-III-COH31 supernatant.

Infection of MΦ monolayers with GBS-III-NEM316, GBS-V-10/84, GBS-Ia-A909, GBS-Ib-H36B, at different cell : microorganism ratios was as described above.

For experiments with calpain inhibitor we added PD150606 (100 μM) to MΦ 1 h before GBS infection and kept during the 2 h infection at the same concentration.

For EGTA experiments, 1 mM was added to MΦ during the 2 h infection and some cultures were added with 1 mM $CaCl_2$ or $MgCl_2$.

For experiments with the intracellular Ca^{2+} chelator, BAPTA/AM, 15 μM BAPTA/AM was added to MΦ 1 h before GBS infection and kept during the 2 h infection.

For experiments with caspase inhibitor, BAF (25 μM) was added to MΦ 2 h before GBS infection and kept during the 2 h infection.

For experiments with other protease inhibitors, CA-074 Me (10 μM), NH_4Cl (10 mM), *clasto*-Lactacystin (2 μM) or MG132 (5 μM) was added to MΦ 1.5 h before GBS infection and kept during the course of experiments at the same concentrations.

For Pepstatin A experiments, 10 μM was added to MΦ 18 h before GBS infection and kept during the 2 h infection.

For experiments with CHX (10 and 50 μg ml^{-1}) as protein synthesis inhibitor and with STS (63 nM) as protein kinase inhibitor, the inhibitors were added to MΦ 1 h before GBS infection and kept during the 2 h infection.

For experiments with simultaneously treatment with proteasome inhibitor and protein synthesis inhibitor, *clasto*-Lactacystin (2 μM) and CHX (50 μg ml^{-1}) were added to MΦ 1.5 h before GBS infection and kept during the course of experiments at the same concentrations.

Controls were MΦ treated with each inhibitor under the same conditions (time and concentration) as GBS-infected MΦ, but not infected.

For DPPC experiments, 2 mg ml^{-1} in PBS of sonicated DPPC (1 min, 30 W) was added to GBS for 5 min before infection with MΦ. Controls were MΦ treated with DPPC in the same condition as infected MΦ but not infected.

Dose response experiments evaluating calpain activity and gelsolin in GBS-infected MΦ, and cell viability in control MΦ showed that in our cellular model: (i) the IC50 for PD150606 is 40 μM, and the maximal concentration of inhibitor tolerated is 125 μM; (ii) the IC50 for BAF is 12 μM, and the maximal concentration of inhibitor tolerated is 30 μM. While for STS (as protein kinase inhibitors), CA-074 Me, Pepstatin A, NH_4Cl, MG132, *clasto*-Lactacystin since these inhibitors did not affect gelsolin increase, dose response experiments were performed in control MΦ, evaluating cell viability by the Trypan blue exclusion method after incubation with serial dilutions of each inhibitor for different times. The results obtained showed that, 200 nM STS, 50 μM for CA-074 Me, 10 μM for Pepstatin A, 10 mM for NH_4Cl, 5 μM for MG132, and 2 μM for *clasto*-Lactacystin are the maximal concentrations of inhibitor tolerated and can be used in MΦ without affecting cell viability, which remained at 98% as evaluated by Trypan blue assay. The effectiveness of the dose of BAF (25 μM) and *clasto*-Lactacystin (2 μM) used in MΦ was previously demonstrated evaluating respectively caspase activity and proteosome activity (Fettucciari *et al.*, 2006). The effectiveness of the dose of CHX (10 and 50 μg ml^{-1}) as de novo synthesis inhibitor has been previously demonstrated (Fettucciari *et al.*, 2000). Therefore, the doses were chosen taking account of inhibitor specificity and cytotoxicity. PD150606, CA-074 Me, Pepstatin A, STS, MG132 and BAPTA/AM, were dissolved in dimethylsulfoxide at a concentration 400 times greater than the final concentration used. This dilution (1:400) in medium showed no vehicle toxic effect. The different times of MΦ pre-incubation with different inhibitors were necessary to achieve the maximum inhibitor effect.

PI uptake assay

At different times, infected and control MΦ were recovered from monolayers as described above, washed, adjusted to

1×10^6 ml^{-1} in PBS containing PI (5 μg ml^{-1}), incubated at 23°C for 5 min and analysed on an EPICS XL-MCL flow cytometer (Instrumentation Laboratory, Beckman Coulter, Miami, FL). Data were processed by an Intercomp computer and analysed with SYSTEM II software (Instrumentation Laboratory, Beckman Coulter).

Total cell lysis and cytoskeleton subcellular fractionation

Control MΦ monolayers and GBS-infected MΦ monolayers (3×10^6 cells/well; 12×10^6 cells/sample) at different times after infection, inhibitor-treated MΦ monolayers and inhibitor-treated GBS-infected MΦ monolayers (3×10^6 cells/well; 12×10^6 cells/sample) at different times after infection, control MΦ monolayers and MΦ monolayers treated with STS (5 μM) or CHX (200 μg ml^{-1}) (3×10^6 cells/well; 12×10^6 cells/sample) for 2 h, were scraped into 100 μl well of a modified RIPA lysis buffer (50 mM Tris-HCl, pH 7.4, 150 mM NaCl, 1% Triton X-100, 1% sodium deoxycholate, 2 mM EDTA, 0.1% SDS, 20 mM β-glycerophosphate, 1 mM PMSF, 10 μg ml^{-1} leupeptin, 10 μg ml^{-1} aprotinin, 1 mM sodium orthovanadate, 1 μg ml^{-1} Pepstatin A, 10 mM benzamidine and 10 mM sodium fluoride, Sigma) on ice and clarified by centrifuging at 16 000 *g* for 15 min at 4°C.

Cytoskeleton purification and subfractionation of cytoskeletal, soluble and nuclear proteins was achieved by the EMD Millipore ProteoExtract Cytoskeleton Enrichment and isolation Kit (Millipore, Billerica, MA) that also contains antibodies (vimentin, GAPDH) for loading control of subcelluar fractions (Millipore). Cytoskeletal, soluble and nuclear fraction from control MΦ monolayers and GBS-infected MΦ monolayers (3×10^6 cells/well; 12×10^6 cells/sample) in 6-well plates, at 1 and 2 h after infection, were prepared using EMD Millipore ProteoExtract Cytoskeleton Enrichment and isolation Kit based on the manufacturer's protocol.

Protein content was determined by a standard Bradford protein assay (Bio-Rad Laboratories, Milan, Italy).

Western blot analysis

Proteins (30 μg) were boiled for 5 min at 95°C, separated on 10% SDS-PAGE and electrophoretically transferred to a nitrocellulose membrane. The blots were blocked with 5% milk in Tris-buffered saline plus 0.1% Tween-20 (TBST) for 1 h at room temperature, and then incubated overnight at 4°C with an appropriate dilution of the primary specific Abs. The blots were then washed four times with TBST and incubated for 1 h with the appropriate HRP-conjugated secondary Ab. Immunoreactive bands were developed using ECL. Autoradiography was performed for variable times. Stripping the blots was performed in stripping buffer (0.2 M NaOH in bidistilled water) for 15 min at room temperature and after four washes with TBST the blots were reprobed as described above. β-actin was used as loading control to whole cell lysates. MnSOD was used as loading control to whole cell lysates. Vimentin was used as loading control for the cytoskeletal fraction, and GAPDH as loading control for the soluble and nuclear fraction. Densitometric analysis was performed using Quantity One software (Bio-Rad, Milan, Italy).

Protein solubilization and 2-DE analysis

At 2 h after infection, control MΦ monolayers and GBS-infected MΦ monolayers (3×10^6 cells/well; 12×10^6 cells/sample) were washed with PBS and lysed 10 min at 20°C in lysis buffer (7 M urea, 2 M thiourea, 2% CHAPS, 40 mM Tris base, 65 mM DTT) supplemented with protease inhibitor cocktail. Disrupted cell suspensions were recovered and proteins were solubilized by tip-sonication at 0°C (4×20 s), followed by vigorous stirring for 18 h at 4°C. The resulting suspensions were centrifuged for 15 min at 12 000 *g* at 4°C. Aliquots of each supernatant were frozen and stored at −80°C till the next analyses. Protein content was quantified by Bradford. Three separate preparations of control MΦ monolayers and GBS-infected MΦ monolayers were solubilized as described above and used for 2-DE analysis. Then each protein sample was analysed in triplicate by 2-DE, producing a total of six replicate gels for each of the following groups: control MΦ (MΦ) and GBS-infected MΦ (MΦ: GBS-III-COH31).

2-DE analysis of 2-DE images using the PDQuest software (version 7.2, Bio-Rad, Hercules, CA, USA), polypeptide identification after separation of Oligopeptides using a ProteomeX apparatus (Thermo Electron, San Jose, CA, USA) and electrospraying of eluted oligopeptides directly into the LCQ Deca-XP^{Plus} ion-trap mass spectrometer, and finally database searching of protein sequence using the MASCOT software version 2.2 (http://www.matrixscience.com/) were performed as previously described (Susta *et al.*, 2010).

qRT-PCR

We used qRT-PCR (Fettucciari *et al.*, 2006) to quantify the expression of mouse genes by using the following sense and antisense primers: gelsolin: 5′-tgctgccatctttactgtgc-3′ and 5′-ctctggaccaccacctcatt-3′; β-actin: 5′-gctcttttccagccttcctt-3′ and 5′-cttctgcatcctgtcagcaa-3′; GAPDH: 5′-ctgagtatgtcgtggagtctac-3′ and 5′-gttggtggtgcaggatgcattg-3′. All PCR primers were designed using PRIMER3-OUTPUT software using published sequence data from the NCBI database. Total RNA was isolated (TRIzol reagent-Invitrogen): (i) for gelsolin expression experiments, from control MΦ and MΦ infected with GBS-III-COH31 at a 1:100 ratio; (ii) for analysing the gelsolin knockdown, from MΦ non-transfected, MΦ mock transfected, MΦ transfected with non-targeting siRNA, MΦ transfected with gelsolin siRNA at 72 post transfection. Purified RNA (1 μg) was treated with DNaseI (Invitrogen, Carlsbad, CA) and then the RNA was reverse transcribed with Superscript II (Invitrogen) in 20 μl reaction volume using random primers. For qRT-PCR, a 25 ng template was dissolved in 25 μl containing 0.2 μmol l^{-1} of each primer, 12.5 μl of Platinum 2× SYBR Green qPCR SuperMix-UDG and 0.5 μl of ROX Reference Dye (Invitrogen). All reactions were performed in triplicate. The thermal cycling conditions were as follows: 2 min at 50°C, 10 min at 95°C, followed by 45 cycles at 95°C for 15 s and 60°C for 1 min in GeneAmp 5700 Sequence Detection System (Applied Biosystem). The fluorescence emission data for each sample were processed using GeneAmp 5700 SDS Software (Applied Biosystem). The mean value of the replicates for each sample was calculated and expressed as the cycle threshold (Ct; cycle number at which each PCR reaction reaches a predetermined fluorescence threshold, set within the linear range of all reactions).

The amount of gene expression was then calculated as the difference (ΔCt) between the mean Ct value of the sample for the target gene and the mean Ct value of that sample for the housekeeping gene, β-actin or GAPDH. The relative expression was calculated as the difference (ΔΔCt) between the ΔCt value of the GBS-infected MΦ versus ΔCt value of control MΦ, or as the difference (ΔΔCt) between the ΔCt value of the transfected cells versus ΔCt value of non-transfected cells. The relative expression level was expressed as $2^{-\Delta\Delta Ct}$ (Fettucciari *et al*., 2006).

Immunofluorescence and phalloidin staining

MΦ (2×10^6) were allowed to adhere on coverslips immersed in 6-well plates for 90 min and then non-adherent cells were removed. After 18 h, MΦ monolayers treated or not with 1 mM EGTA, MΦ monolayers pretreated or not with 100 μM PD150606, were infected for 2 h with GBS-III-COH31, as described above, in presence or absence of the EGTA or calpain inhibitor. After PBS washes, the cells were fixed for 20 min with 4% paraformaldehyde, permeabilized with 0.1% Triton X-100 for 10 min, and after washing in PBS containing 0.05% Triton X-100 (PBSTr) incubated in blocking buffer (PBSTr containing 2.5% BSA) for 30 min. The primary monoclonal mouse anti-gelsolin Ab (1:100) in blocking buffer was added and incubated for 1 h. Then Alexa Fluor 568-labelled goat anti-mouse IgG Ab, to detect gelsolin was added at a 1:200 dilution. Alexa Fluor 488 phalloidin was used to detect F-actin. DAPI was added at 1 μg ml^{-1} to counterstain nuclei. The coverslips were mounted on microscopic glass slides with ProLong Gold antifade medium. All steps were performed at room temperature.

Fluorescence was evaluated by confocal microscopy (Nikon Instruments, Amsterdam, Netherlands, C1 on Eclipse Ti; EZC1 software) fitted with an argon laser (488 nm excitation), a He/Ne laser (542 nm excitation) and UV excitation at 405 nm (DAPI staining) from a blue diode.

Apoptosis evaluation

GBS-infected MΦ, control MΦ, MΦ treated with STS (5 μM), or MΦ treated with CHX (200 μg ml^{-1}) were recovered at different times to detect apoptosis (Fettucciari *et al*., 2000). The cell pellets were resuspended in 1 ml hypotonic fluorochrome solution (PI 50 μg ml^{-1} in 0.1% sodium citrate plus 0.1% Triton X-100). Samples were placed overnight in the dark at 4°C, and the PI fluorescence of individual nuclei measured using a EPICS XL-MCL flow cytometer (Instrumentation Laboratory, Beckman Coulter). Data were processed by an Intercomp computer and analysed with SYSTEM II software (Instrumentation Laboratory, Beckman Coulter).

siRNA transfection

siRNA transfection was performed as previously described (Fettucciari *et al*., 2006) and according to the manufacturer's protocol for Lipofectamine 2000 (Invitrogen). Briefly, 100 nM siRNA specific for the mouse gelsolin and the control non-targeting siRNA were solubilized in the appropriate amount of RPMI-1640 without serum and mixed gently. Lipofectamine 2000 was mixed gently, then diluted in the appropriate amount of RPMI-1640 without serum, mixed gently and incubated at room temperature. After 5 min incubation, the diluted siRNA were combined with the diluted Lipofectamine 2000, mixed gently and incubated for 20 min to allow complex formation. The siRNA-Lipofectamine complexes were added to the cultured MΦ seeded 18 h before in a 6-well plate at 70–80% cell confluence. The plates were mixed gently by rocking back and forth and incubated for 72 h a 37°C 5% CO_2. In mock transfection, all vehicles were used except for the siRNA. Cell vitality was monitored continuously throughout the experiments. 98% cells were vital during the course of all experiments as determined by Trypan blue exclusion assay. At 72 h post transfection the effect of siRNA was evaluated analysing the gelsolin knockdown by measuring the relative expression of gelsolin gene versus GAPDH by qRT-PCR. Furthermore at 72 h post transfection the cells were washed, placed in fresh RPMI and infected with GBS-III-COH31 as described above and then apoptosis performed as described above.

Statistical analysis

Data of apoptosis and PI uptake assay are presented as the means ± Standard Deviation (SD) of six independent experiments performed in triplicate. Western blot analysis was repeated in three or four independent experiments and representative blots are shown. Experiments of silencing by siRNA assay were repeated four times. Confocal microscopy was repeated three times and representative images are shown. The data were analysed by Student's *t*-test.

Acknowledgements

The authors thank Catherine Bennett Gillies for the excellent assistance in preparing the manuscript. This work was supported by a grant from Fondazione Cassa di Risparmio di Perugia, Italy (bando 2010 – 2010.020.0131 Ricerca Scientifica e Tecnologica; K.F.) and PRIN (Anno 2008 – prot. 2008L57JXW_003; K.F.)

Disclosures

No conflict of interest for all the authors.

References

Arcaro, A. (1998) The small GTP-binding protein Rac promotes the dissociation of gelsolin from actin filaments in neutrophils. *J Biol Chem* **273:** 805–813.

Areschoug, T., Waldemarsson, J., and Gordon, S. (2008) Evasion of macrophage scavenger receptor A-mediated recognition by pathogenic streptococci. *Eur J Immunol* **38:** 3068–3079.

Ashish, Paine, M.S., Perryman, P.B., Yang, L., Yin, H.L., and Krueger, J.K. (2007) Global structure changes associated with Ca2+ activation of full-length human plasma gelsolin. *J Biol Chem* **282:** 25884–25892.

Azuma, T., Witke, W., Stossel, T.P., Hartwig, J.H., and Kwiatkowski, D.J. (1998) Gelsolin is a downstream effector of rac for fibroblast motility. *EMBO J* **17:** 1362–1370.

Azuma, T., Koths, K., Flanagan, L., and Kwiatkowski, D. (2000) Gelsolin in complex with phosphatidylinositol 4,5-

bisphosphate inhibits caspase-3 and -9 to retard apoptotic progression. *J Biol Chem* **275:** 3761–3766.

Baker, C.J., and Edwards, M.S. (1995) Group B streptococcal infections. In *Infectious Diseases of the Fetus and Newborn Infant*, 4th edn. Remington, J., and Klein, J.O. (eds). Philadelphia, PA: The WB Saunders Co, pp. 980–1054.

Belyi, I.F. (2002) Actin machinery of phagocytic cells: universal target for bacterial attack. *Microsc Res Tech* **57:** 432–440.

Benjamins, J.A., Nedelkoska, L., and George, E.B. (2003) Protection of mature oligodendrocytes by inhibitors of caspases and calpains. *Neurochem Res* **28:** 143–152.

Bhatia, V., Mula, R.V., and Falzon, M. (2013) Parathyroid hormone-related protein regulates integrin $\alpha 6$ and $\beta 4$ levels via transcriptional and post-translational pathways. *Exp Cell Res* **319:** 1419–1430.

Brochet, M., Couvé, E., Zouine, M., Vallaeys, T., Rusniok, C., Lamy, M.C., *et al.* (2006) Genomic diversity and evolution within the species Streptococcus agalactiae. *Microbes Infect* **8:** 1227–1243.

Carafoli, E., and Molinari, M. (1998) Calpain: a protease in search of a function? *Biochem Biophys Res Commun* **247:** 193–203.

Ciechanover, A. (1998) The ubiquitin-proteasome pathway: on protein death and cell life. *EMBO J* **17:** 7151–7160.

Cornacchione, P., Scaringi, L., Fettucciari, K., Rosati, E., Sabatini, R., Orefici, G., *et al.* (1998) Group B streptococci persist inside macrophages. *Immunology* **93:** 86–95.

Cossart, P. (2004) Bacterial invasion: a new strategy to dominate cytoskeleton plasticity. *Dev Cell* **6:** 314–315.

Cossart, P., and Sansonetti, P.J. (2004) Bacterial invasion: the paradigms of enteroinvasive pathogens. *Science* **304:** 242–248.

Coux, O., Tanaka, K., and Goldberg, A.L. (1996) Structure and functions of the 20S and 26S proteasomes. *Annu Rev Biochem* **65:** 801–847.

Croons, V., Martinet, W., Herman, A.G., Timmermans, J.P., and De Meyer, G.R. (2007) Selective clearance of macrophages in atherosclerotic plaques by the protein synthesis inhibitor cycloheximide. *J Pharmacol Exp Ther* **320:** 986–993.

De Corte, V., Bruyneel, E., Boucherie, C., Mareel, M., Vandekerckhove, J., and Gettemans, J. (2002) Gelsolin-induced epithelial cell invasion is dependent on Ras-Rac signaling. *EMBO J* **21:** 6781–6790.

Donovan, M.J., Maciuba, B.Z., Mahan, C.E., and McDowell, M.A. (2009) Leishmania infection inhibits cycloheximide-induced macrophage apoptosis in a strain-dependent manner. *Exp Parasitol* **123:** 58–64.

Fettucciari, K., Rosati, E., Scaringi, L., Cornacchione, P., Migliorati, G., Sabatini, R., *et al.* (2000) Group B Streptococcus induces apoptosis in macrophages. *J Immunol* **165:** 3923–3933.

Fettucciari, K., Fetriconi, I., Bartoli, A., Rossi, R., and Marconi, P. (2003) Involvement of mitogen-activated protein kinases in Group B Streptococcus-induced macrophage apoptosis. *Pharmacol Res* **47:** 355–362.

Fettucciari, K., Fetriconi, I., Mannucci, R., Nicoletti, I., Bartoli, A., Coaccioli, S., and Marconi, P. (2006) Group B Streptococcus induces macrophage apoptosis by calpain activation. *J Immunol* **176:** 7542–7556.

Fettucciari, K., Quotadamo, F., Noce, R., Palumbo, C., Modesti, A., Rosati, E., *et al.* (2011) Group B Streptococcus (GBS) disrupts by calpain activation the actin and microtubule cytoskeleton of macrophages. *Cell Microbiol* **13:** 859–884.

Gargalovic, P., and Dory, L. (2003) Cellular apoptosis is associated with increased caveolin-1 expression in macrophages. *J Lipid Res* **44:** 1622–1632.

Gibson, R.L., Redding, G.J., Truog, W.E., Henderson, W.R., and Rubens, C.E. (1989) Isogenic group B streptococci devoid of capsular polysaccharide or beta-haemolysin: pulmonary hemodynamic and gas exchange effects during bacteremia in piglets. *Pediatr Res* **26:** 241–245.

Glaser, P., Rusniok, C., Buchrieser, C., Chevalier, F., Frangeul, L., Msadek, T., *et al.* (2002) Genome sequence of Streptococcus agalactiae, a pathogen causing invasive neonatal disease. *Mol Microbiol* **45:** 1499–1513.

Goll, D.E., Thompson, V.F., Li, H., Wei, W., and Cong, J. (2003) The calpain system. *Physiol Rev* **83:** 731–801.

Groves, E., Dart, A.E., Covarelli, V., and Caron, E. (2008) Molecular mechanisms of phagocytic uptake in mammalian cells. *Cell Mol Life Sci* **65:** 1957–1976.

Hensler, M.E., Miyamoto, S., and Nizet, V. (2008) Group B streptococcal beta-haemolysin /cytolysin directly impairs cardiomyocyte viability and function. *PLoS ONE* **3:** e2446.

Jänicke, R.U., Ng, P., Sprengart, M.L., and Porter, A.G. (1998) Caspase-3 is required for alpha-fodrin cleavage but dispensable for cleavage of other death substrates in apoptosis. *J Biol Chem* **273:** 15540–15545.

Ji, L., Chauhan, A., and Chauhan, V. (2010) Calcium induces expression of cytoplasmic gelsolin in SH-SY5Y and HEK-293 cells. *Neurochem Res* **35:** 1075–1082.

Kiselar, J.G., Janmey, P.A., Almo, S.C., and Chance, M.R. (2003) Visualizing the Ca+ 2-dependent activation of gelsolin by using synchrotron footprinting. *Proc Natl Acad Sci USA* **100:** 3942–3947.

Kothakota, S., Azuma, T., Reinhard, C., Klippel, A., Tang, J., Chu, K., *et al.* (1997) Caspase-3-generated fragment of gelsolin: effector of morphological change in apoptosis. *Science* **278:** 294–298.

Koya, R.C., Fujita, H., Shimizu, S., Ohtsu, M., Takimoto, M., Tsujimoto, Y., and Kuzumaki, N. (2000) Gelsolin inhibits apoptosis by blocking mitochondrial membrane potential loss and cytochrome c release. *J Biol Chem* **275:** 15343–15349.

Kusano, H., Shimizu, S., Koya, R.C., Fujita, H., Kamada, S., Kuzumaki, N., and Tsujimoto, Y. (2000) Human gelsolin prevents apoptosis by inhibiting apoptotic mitochondrial changes via closing VDAC. *Oncogene* **19:** 4807–4814.

Kwiatkowski, D.J. (1999) Functions of gelsolin: motility, signaling, apoptosis, cancer. *Curr Opin Cell Biol* **11:** 103–108.

Li, G.H., Arora, P.D., Chen, Y., McCulloch, C.A., and Liu, P. (2012) Multifunctional roles of gelsolin in health and diseases. *Med Res Rev* **32:** 999–1025.

Liu, G.Y., Doran, K.S., Lawrence, T., Turkson, N., Puliti, M., Tissi, L., and Nizet, V. (2004) Sword and shield: linked group B streptococcal beta-haemolysin/cytolysin and carotenoid pigment function to subvert host phagocyte defense. *Proc Natl Acad Sci USA* **5:** 14491–14496.

McGhie, E.J., Hayward, R.D., and Koronakis, V. (2004) Control of actin turnover by a salmonella invasion protein. *Mol Cell* **13:** 497–510.

McGough, A.M., Staiger, C.J., Min, J.K., and Simonetti, K.D. (2003) The gelsolin family of actin regulatory proteins: modular structures, versatile functions. *FEBS Lett* **552:** 75–81.

Maisey, H.C., Doran, K.S., and Nizet, V. (2008) Recent advances in understanding the molecular basis of group B Streptococcus virulence. *Expert Rev Mol Med* **10:** e27.

Marchlewicz, B.A., and Duncan, J.L. (1980) Properties of a haemolysin produced by group B streptococci. *Infect Immun* **30:** 805–813.

May, R.C., and Machesky, L.M. (2001) Phagocytosis and the actin cytoskeleton. *J Cell Sci* **114:** 1061–1077.

Melendez, A.J., and Tay, H.K. (2008) Phagocytosis: a repertoire of receptors and Ca(2+) as a key second messenger. *Biosci Rep* **28:** 287–298.

Menconi, M.J., Wei, W., Yang, H., Wray, C.J., and Hasselgren, P.O. (2004) Treatment of cultured myotubes with the calcium ionophore A23187 increases proteasome activity via a CaMK II-caspase-calpain-dependent mechanism. *Surgery* **136:** 135–142.

Nandi, D., Tahiliani, P., Kumar, A., and Chandu, D. (2006) The ubiquitin-proteasome system. *J Biosci* **31:** 137–155.

Ni, X.G., Zhou, L., Wang, G.Q., Liu, S.M., Bai, X.F., Liu, F., *et al*. (2008) The ubiquitin-proteasome pathway mediates gelsolin protein downregulation in pancreatic cancer. *Mol Med* **14:** 582–589.

Nizet, V. (2002) Streptococcal beta-haemolysin s: genetics and role in disease pathogenesis. *Trends Microbiol* **10:** 575–580.

Nizet, V., Gibson, R.L., Chi, E.Y., Framson, P.E., Hulse, M., and Rubens, C.E. (1996) Group B streptococcal beta-haemolysin expression is associated with injury of lung epithelial cells. *Infect Immun* **64:** 3818–3826.

Norberg, E., Gogvadze, V., Ott, M., Horn, M., Uhlén, P., and Zhivotovsky, B. (2008) An increase in intracellular Ca2+ is required for the activation of mitochondrial calpain to release AIF during cell death. *Cell Death Differ* **15:** 1857–1864.

Paolini, R., Molfetta, R., Piccoli, M., Frati, L., and Santoni, A. (2001) Ubiquitination and degradation of Syk and ZAP-70 protein tyrosine kinases in human NK cells upon CD16 engagement. *Proc Natl Acad Sci USA* **98:** 9611–9616.

Patrick, G.N., Zhou, P., Kwon, Y.T., Howley, P.M., and Tsai, L.H. (1998) p35, the neuronal-specific activator of cyclin-dependent kinase 5 (Cdk5) is degraded by the ubiquitin-proteasome pathway. *J Biol Chem* **273:** 24057–24064.

Pillay, C.S., Elliott, E., and Dennison, C. (2002) Endolysosomal proteolysis and its regulation. *Biochem J* **363:** 417–429.

Rabkin, S.W., and Kong, J.Y. (2002) Discordance between the effect of modulators of calcium on staurosporine-induced apoptosis and staurosporine-induced actin degradation. *Cell Biol Int* **26:** 433–440.

Rajagopal, L. (2009) Understanding the regulation of Group B Streptococcal virulence factors. *Future Microbiol* **4:** 201–221.

Rosati, E., Fettucciari, K., Scaringi, L., Cornacchione, P., Sabatini, R., Mezzasoma, L., *et al*. (1998) Cytokine response to group B streptococcus infection in mice. *Scand J Immunol* **47:** 314–323.

Rubens, C.E., Wessel, M.R., Heggen, L.M., and Kasper, D.L. (1987) Transposon mutagenesis of type III group B streptococcus: correlation of capsule expression with virulence. *Proc Natl Acad Sci USA* **84:** 7208–7212.

Sigge, A., Schmid, M., Mauerer, S., and Spellerberg, B. (2008) Heterogeneity of hemolysyn expression during neonatal *Streptoccoccus agalactiae* sepsis. *J Clin Microbiol* **46:** 807–809.

Silacci, P., Mazzolai, L., Gauci, C., Stergiopulos, N., Yin, H.L., and Hayoz, D. (2004) Gelsolin superfamily proteins: key regulators of cellular functions. *Cell Mol Life Sci* **61:** 2614–2623.

Smith, I.J., and Dodd, S.L. (2007) Calpain activation causes a proteasome-dependent increase in protein degradation and inhibits the Akt signalling pathway in rat diaphragm muscle. *Exp Physiol* **92:** 561–573.

Spinardi, L., and Witke, W. (2007) Gelsolin and diseases. *Subcell Biochem* **45:** 55–69.

Susta, F., Chiasserini, D., Fettucciari, K., Orvietani, P.L., Quotadamo, F., Noce, R., *et al*. (2010) Protein expression changes induced in murine peritoneal macrophages by Group B Streptococcus. *Proteomics* **10:** 2099–2112.

Tettelin, H., Masignani, V., Cieslewicz, M.J., Donati, C., Medini, D., Ward, N.L., *et al*. (2005) Genome analysis of multiple pathogenic isolates of Streptococcus agalactiae: implications for the microbial 'pan-genome'. *Proc Natl Acad Sci USA* **102:** 13950–13955.

Toledo, L.M., and Lydon, N.B. (1997) Structures of staurosporine bound to CDK2 and cAPK–new tools for structure-based design of protein kinase inhibitors. *Structure* **5:** 1551–1556.

TranVan Nhieu, G., Clair, C., Grompone, G., and Sansonetti, P. (2004) Calcium signalling during cell interactions with bacterial pathogens. *Biol Cell* **96:** 93–101.

Valentin-Weigand, P., Benkel, P., Rohde, M., and Chhatwal, G.S. (1996) Entry and intracellular survival of group B streptococci in J774 macrophages. *Infect Immun* **64:** 2467–2473.

Valentin-Weigand, P., Jungnitz, H., Zock, A., Rohde, M., and Chhatwal, G.S. (1997) Characterization of group B streptococcal invasion in HEp-2 epithelial cells. *FEMS Microbiol Lett* **147:** 69–74.

Wang, K.K., Nath, R., Posner, A., Raser, K.J., Buroker-Kilgore, M., Hajimohammadreza, I., *et al*. (1996) An alpha-mercaptoacrylic acid derivative is a selective nonpeptide cell-permeable calpain inhibitor and is neuroprotective. *Proc Natl Acad Sci USA* **93:** 6687–6692.

Wilkinson, H.W. (1977) Nontypable group B streptococci isolated from human sources. *J Clin Microbiol* **6:** 183–184.

Zhao, J., Tenev, T., Martins, L.M., Downward, J., and Lemoine, N.R. (2000) The ubiquitin-proteasome pathway regulates survivin degradation in a cell cycle-dependent manner. *J Cell Sci* **23:** 4363–4371.

Zhou, P. (2004) Determining protein half-lives. In *Methods in Molecular Biology: Signal Transduction Protocols*. Dickson, R.C., and Mendenhall, M.D. (eds). Totowa, NJ: Humana Press, pp. 67–77.

Supporting information

Additional Supporting Information may be found in the online version of this article at the publisher's web-site:

Fig. S1. GBS-III-COH31 induction of MΦ apoptosis.

Apoptosis of control MΦ and MΦ infected with GBS-III-COH31 at the indicated ratios was measured at different times after infection evaluating by flow cytometry the percentage of hypodiploid nuclei. Data are means ± SD of six experiments done in triplicate. $^{*}P < 0.01$ GBS-infected MΦ versus control MΦ.